AD 268 338

RADC-TR61-116 ✓ 648800

NUCLEAR CORPORATION OF AMERICA

$5.60

RADC-TR61-116

8/16/61

HIGH POWER PULSE SWITCH TUBE

B Y

B. Bernstein
J. Glauber
H. Koch

NUCLEAR CORPORATION OF AMERICA
Central Electronic Mfr's. Div.
Denville, N. J.

Contract Number
AF30(602)-2027

Prepared For

ROME AIR DEVELOPMENT CENTER
Air Research and Development Command
United States Air Force

Griffiss Air Force Base
New York

ABSTRACT

The design of a 45 megawatt tetrode switch tube with water cooled grids, water cooled anode and matrix cathode is described. The choice of the matrix type cathode was made after consideration was given to all other popular types.

Preliminary experiments which led to the final assembly method are described.

The calculation of the tube characteristics is explained in detail. Drawings and sketches of the various parts, sub-assemblies and assemblies are included.

A simplified proposed design is mentioned.

INTRODUCTION

The purpose of this report is to investigate theoretically and experimentally the various cathode materials and techniques to provide performance prediction criteria, for their use in the construction of a high power pulse switch tube. The investigation includes;

a) Exploratory investigation into the available cathode materials currently in use and also those materials which show promise as suitable electron emitters for use in a high power pulse switch tube.

b) Investigation and evaluation of these cathode materials in various forms including wire cage structures, formed bars, ribbon type, cylindrical sheets and, matrix types.

c) A breadboard model of a switch tube in accordance with the tentative design specification in (f) below.

d) Investigation and evaluation of methods for cooling a tube at the proposed power level.

e) The investigation into the feasibility of incorporating an electrical gettering component which will continuously getter the tube with longer and more efficient tube life as the goal.

f) A tentative design specification which will permit the construction of a high-power switch tube to operate near the following conditions:

	Minimum	Objectives	Unit
(1) Peak Voltage:	40	65	KV
(2) Peak Current:	600	7.50	Amps.
(3) Peak Power:	25	45	Megawatt
(4) Duty:	0.01	0.01	
(5) Pulse Width	7	25	Msecs.

TABLE OF CONTENTS

FINAL REPORT - XD-32

OBJECTIVES:

To fabricate a high power switch tube capable of operating as follows:

1) Peak anode voltage - 75KV
2) Peak anode current - 750 amps
3) Peak power - 45 megawatts
4) Duty cycle - .01
5) Pulse width - 25 microseconds

The method of cooling the various electrodes to be decided after evaluation of power dissipation in each electrode.

THEORETICAL AND EXPERIMENTAL INVESTIGATIONS:

Types of Cathodes: Various types of cathodes were investigated and evaluated as follows:

1) Pure tungsten is impractical
2) Thoriated tungsten would require an area of 400 sq. cm to deliver 1125 amperes of cathode current (on the basis of 750 amperes of plate current and 375 amperes of grid current). The power required for the cathode would be 11.25KW on the basis of 100 mAmps of emission per watt of cathode power. This plus the mechanical difficulties of a filamentary type of cathode makes it highly undesirable.
3) The oxide coated group which covers a wide variety includes the standard nickel sleeve, spray coated with barium and

strontium carbonates as well as the matrix or impregnated type. The latter, briefly, consists of a refractory metal sleeve (molybdenum, tungsten, tantalum, or rhenium) with a layer of nickel powder sintered to the outer surface. The porous layer is then saturated with a suspension of the carbonates. On the basis of 5 amps/sq. cm peak current, which is a reasonable figure with a total peak cathode current of 1125 amperes, a cathode area of 225 sq. cm will be required. The heater power required on the basis of one watt per ampere of cathode current is 1.125KW.

4) The dispenser cathode which is porous tungsten with the pores filled with barium aluminate warrants investigation because of its resistance to sparking and positive ion bombardment. This type of cathode will permit of 8 amps/sq. cm with an emissive area of 140 sq. cm. The heater power required would be 2.27KW which is still not unreasonable. One objection to this cathode is the fact that it cannot be obtained in very large sizes.

5) The thoria bonded cathode is only about ten percent better than thoriated tungsten.

This survey then narrows down the field to two types, matrix or impregnated. This in itself isn't so much

a choice of cathodes as it is a choice of materials.

Experimental work was started on the matrix type which consisted of carbonyl nickel powder sintered to a molybdenum base metal. Very poor adherence resulted until the molybdenum was acid etched. This type of filamentary cathode is shown in Figure 1 and the test results are shown in Figure 2. The operating current of the filament was calculated to be 48 amperes, but the addition of the sintered niclel powder changes the conductivity considerably requiring almost twice as much current. The matrix cathode is not particularly suited for directly heated emitters.

The difficulties encountered in sintering the nickel to a refractory base and the success some people have had with pressed and sintered cathodes of 70% nickel and 30% barium-strontium carbonates lead to the possibility of cataphoretically coating a refractory metal wire with such a mixture. Since the nickel powder does not stay in suspension very well, it was thought that a mixture of 70% nickel oxide and 30% double carbonate might be tried. The coated cathode would then be fired in hydrogen at 1050°C. A tungsten filament was coated in this fashion with the results shown in figure 3. From this data it is seen that 10 amps/sq. cm

are easily obtained and that practical cathodes can be made in this fashion. The apparent success of sintering the nickel powder on a nickel sleeve made this technique obsolete. The latest development has been the availability of porous nickel by the Mott Engineering Company.

The dispenser type was investigated through Semicon Associates. Dr. O. G. Koppius, who heads the company, informed us that tubes operating on CW have run current densities of 8 amps/sq. cm. In pulse operation they have obtained 15-20 amps/sq. cm with a pulse width of 60 u sec. at 60 pps and felt that this was not the upper limit. Accordingly, several cathodes were ordered of a size that would be used in the final tube. The cathodes were to be cut into strips, but this was never successfully accomplished. A fragment was investigated in the bell jar with the conclusion that as a directly heated cathode it was extremely inefficient as shown in Figure 4. The recommended temperature of 1050°C requires about 82.5 amperes. Mounting the material so that it can be indirectly heated poses so many problems that this form of cathode was abandoned in favor of the matrix cathode.

Electrode Configurations: Originally it was claimed that a beaming structure was required such as the Resnatron (IRE Proceedings, Aug. 1958) a Pierce gun (J. Applied Physics, Aug. 1940)

or a combination of the two. A preliminary design was worked out utilizing parts of both of the above systems and is shown in Figure 5. The grid and screen rods, in conjunction with the curved cathode, results in an approximation of a Pierce type gun. This approximation occurs when the grid potential is at its peak positive value and has a particular value in relation to the screen potential. The potential along the beam must vary as the 4/3 power of the distance. Since the screen is fixed in potential, the best beam formation will occur when E_{G1} is 0.31 E_{G2} for the dimensions shown in Figure 5. The general theory has been checked on the type 3D21A, which is a beam power tube. The published data was replotted as shown in Figure 6, i.e. plate, screen, and control grid currents plotted as a function of control grid voltage. The ratio of total grid current to plate current was calculated and is plotted in per cent. It is seen that at about 120 volts on the control grid that the ratio of total grid current to plate current is beginning to increase at a greater rate. Measurements on several tubes give control grid to cathode spacing of 0.012" and screen grid to cathode spacing of 0.042. For these spacings and a screen potential of 800 volts, the control grid should be 0.148 E_{C2} or 126.4 volts for optimum "focus". This would seem to be good agreement between theory and practice.

In order to get some measure of how closely Design #1 (Figure 5) would come to the above theory, some approximations were made. Since the spacing between cathode and grid is small compared to the radius of the cathode, the configuration is essentially planar. Having a flat cathode rather than a concave surface should not introduce a serious error in the light of the above calculations. Three sections have been set up with only the center cathode emitting, the outer ones being used to maintain potential distribution. This and subsequent changes in design shown in Figure 8 were tested in a bell jar system.

The results of the initial layout, Des. 1, are shown in Figure 9. There is good agreement between measured and calculated diode characteristics in this and subsequent designs. The perveance determined from measured values is 0.026 $mA/V^{3/2}$ for a cathode area of 1.22 sq. cm. The perveance will increase directly with the cathode area and for 200 sq. cm cathode area, the perveance would be 4.25×10^{-3} $amps/V^{3/2}$ which makes allowance for grid and screen currents and will yield 750 amps of plate current at 6500 volts on grid, screen, and plate. It is seen that this first design is adequate as far as perveance is concerned. Analysis of the tetrode characteristics, though, indicated need for improvement.

Originally we considered the cathode, grid rods, and screen rods as elements of a Pierce gun. For the potential on the screen (300 volts) and the location of the grid and screen rods, the voltage on the control grid for optimum focus should be 93 volts. The optimum focus is considered to be the point where the grid currents ($I_{C1} \neq I_{C2}$) to plate current ratio is a minimum or essentially flat. For Des. 1, the minimum ratio occurs at about 20 volts which does not agree with the theoretical value very well. Beyond this point the grid currents increase at a greater rate than the plate current, and it would be desirable to have the optimum grid potential at a more positive value. This can be accomplished by decreasing the grid to cathode spacing.

The results of smaller grid to cathode spacing are shown in Figure 10, for Des. 1, Rev. 1. This also increases the perveance to .035 $mA/V^{3/2}$. Examination of the tetrode characterictics shows the optimum grid voltage to be about 48 volts, the calculated value is 112 volts. The optimum grid voltage has been shifted to the right but at the same time the ratio of grid current to plate current has increased considerably. From these results it was concluded that the ratio of grid rod pitch (p) and grid to cathode spacing (Z_{G1}) was too low.

The ratio p/Z_{G1} can be conveniently increased by decreasing the width of the cathode as was done in Des. 2, the results of

which are shown in Figure 11. Since the grid to cathode spacing was reduced still more, the perveance has increased considerably viz. 0.107 mA/$V^{3/2}$. The ratio of grid to plate current has deteriorated still further and there is no indication of an optimum grid voltage. For comparison of this design with the previous one, operation of Des. 1, Rev. 1 at 400 volts on the screen and plate has been plotted on Figure 11 too. From these results it was concluded that the grid pitch to grid rod diameter must also be considered and that focusing with the grid voltage is purely secondary if at all pertinent.

The ratio of grid pitch to cathode width was increased in Des. 3 with little change in perveance as shown in Figure 12, but examination of the tetrode characteristics shows a definite improvement in grid to plate current ratio.

The conclusion drawn from these tests were that the grid pitch should be increased materially and the grid to cathode spacing should be increased too. The grid to cathode spacing should not be increased beyond 0.100" because this yields a perveance of .035mA/$V^{3/2}$ for a cathode area of 1.22 sq. cm. For a cathode area of 200 sq. cm. the perveance would be 5.7 x 10^{-3} amps/$V^{3/2}$ which would be more than enough for the final tube. The optimum grid pitch will have to be modified by practical factors.

A total emissive area of 200 sq. cm. should be sufficient for the peak current requirements. The length of the cathode should be about 9 cm long as a practical maximum. The number of emissive sections was chosen as 50, which yields an area of 4 sq. cm for each section. The width of each section is then 0.444 cm (0.175") for a 9cm length. Assuming ideal conditions, a beam of this width (0.175") plus a clearance of 0.030" between beam and grid rod of 0.060" diameter yields a grid rod pitch of 0.295". This then yields a grid rod pitch to grid rod diameter ratio of 4.9. The ratio for Des. 3 was 2.9 and for the 3D21A it is 5.56.

The cathode in Des. 4 then is 0.44 cm wide and 3 cm long which is 1/3 the length of the final cathode. The results are shown in Figure 13, which when compared with Des. 3 (Figure 12) show a considerable improvement in tetrode operation. These data were then extrapolated to determine the characteristics of the final tube.

For a planar design, the perveance is given by:

$$G_o = 3.62 \frac{WL}{Z_{G1}^2} \qquad mA/V^{3/2}$$

where W = cathode width in mm.,

L = cathode length in mm,

Z_{G1} = cathode to grid spacing in mils.

For the model of Des. 4, the perveance is calculated to be 0.052 $mA/V^{3/2}$.

The perveance obtained from the diode characteristic in Figure 13 is 0.043 $mA/V^{3/2}$ (43 mA at 100 volts).

One section in the final tube will have three times the area that one section in the model has and also three times the perveance viz. 0.56×10^{-3} $amps/V^{3/2}$ (Calculated value).

Only one other factor is needed to calculate the final tube characteristics, and that is the amplification factor, μ. This can be calculated from a number of formulas or as in this case it was obtained from Jervis' Chart (E.R. Jervis, Amplification Factor Chart, Electronics, Vol. 12, p. 45, June 1939) and is 4. This is the triode amplification factor, i.e. from control grid to screen and the tetrode amplification factor will be many times this factor but is not pertinent to the calculation of total cathode current. In the positive grid region, the control grid is the principal factor in determining the cathode current and the screen exercises a lesser role. The cathode current is given by the following expression:

$$I_K = G_o \left[\frac{E_{C1} + \frac{E_{C2}}{\mu}}{1 + \frac{1}{\mu}} \right]^{3/2}$$

and for one section:

$$I_K = 0.156 \times 10^{-3} \left[\frac{E_{C1} + \frac{E_{C2}}{4}}{1.25} \right]^{3/2} \quad \text{amps.}$$

The distribution of the cathode current between the various elements is given by Figure 14. This results from the plotting of control grid, screen grid and plate currents as percentages of the cathode current vs. the ratio of control grid and screen grid voltages for a wide range of screen grid voltage. This is another way of saying that the current distribution in a tetrode is constant if the potential distribution is constant. In all of this discussion it is assumed that the anode is at the screen potential or not too much below it, otherwise we get into difficulties with secondary emission and instability results.

The cathode current for one section was calculated for 6000 volts on the screen as a function of positive control grid voltage. The results are shown in Figure 15. It is seen that 15 amperes of plate current are obtainable at about 1700 volts on the grid. For the total 50 sections, the total plate current will be 750 amperes.

A plate family of tho final tube is shown in Figure 16 and covers the positive grid region. For 6000 volts on the screen and triode amplification factor of 4, the cutoff will be about -1500 volts.

For the load line drawn on the plate family the following conditions are obtained:

Plate Supply Voltage - - - - - - - - - - - - - - - - - - - 65KV

Screen Grid Voltage - - - - - - - - - - - - - - - - - - - 6KV

Grid Bias, Cutoff -	1.5KV
Grid Drive Voltage, Max. - - - - - - - - - - - - - - - - -	1.7KV
Plate Voltage, Min. -	6KV
Peak Plate Current -	750 Amps
Peak Screen Grid Current - - - - - - - - - - - - - - - - -	150 Amps
Peak Control Grid Current - - - - - - - - - - - - - - - - -	112 Amps
Peak Plate Dissipation - - - - - - - - - - - - - - - - -	4500KW
Peak Screen Grid Dissipation - - - - - - - - - - - - - -	900 KW
Peak Control Grid Dissipation - - - - - - - - - - - - -	190KW
For .01 duty cycle -	
Average Plate Dissipation - - - - - - - - - - - - - - - -	45KW
Average Screen Grid Dissipation - - - - - - - - - - - -	9KW
Average Control Grid Dissipation - - - - - - - - - - -	1.9KW

The cooling requirements will be dealt with later; at the moment it would be well to complete the discussion of the fundamental design. To confirm the geometry of the tube, an electrolytic tank was constructed, and scale models were studied therein.

Figure 17 shows the equipotential lines for plate and screen at the same potential and the control grid at 25% of the screen and plate potential. Flux lines have been sketched in for the right side of the cathode and all terminate at the grid rod. The flux lines define the electron trajectories indicating that under these conditions the control grid would collect about 50%

of the cathode current. The screen will collect a good portion too. This confirms the results of Des. 3 (fig. 12) that were obtained on scaled models in the bell jar.

Figure 18 shows the results on Des. 4 with the equipotential lines for plate and screen at the same potential and the control grid at 40% of the screen potential. The equipotential lines are much flatter between cathode and grid than they are for Des. 3 even though the grid voltage is more positive. This confirms the data obtained in the bell jar and shown on Figure 13 which indicated that the control grid could be driven positive to 30% to 40% of the screen potential without losing too much current to the grids.

The question of whether or not the curved cathode was necessary was never answered in the bell jar because of the difficulties in making a curved cathode. Because of this a flat cathode was investigated and is also shown on Figure 18. The only effect of the flat cathode is to push the equipotential lines outward because the cathode on the average is closer to the control grid. From these data it can be concluded that a curved cathode is not necessary.

Figure 19 shows a comparison of round and flat screen rods and the effect is to further reduce the screen current. This can be deduced from the fact that the equipotential lines are

pushed out slightly and the electrons will be deflected later and more of them will miss the screen.

The question as to whether a grounded or positive screen will give better operation is partly answered by Figure 20. Good operation with grounded screen can be obtained by driving the grid positive to about 90% of the plate voltage. This is about three times the voltage required when the screen is positive.

The advantage of the grounded screen lies in the fact that there is no screen dissipation, but the driving power for the control grid is increased considerably. The grid dissipation is 1.9KW average and the screen dissipation is 9KW. Since the screen dissipation is higher than the control grid, then if cooling is adequate for the former, it will be adequate for the latter. The screen grid consists of 25 hairpin shaped nickel tubes, .060 O.D. x 040 I.D. and approximately 16 inches long. Each section dissipates 180 watts over an active or "hot" section of 6 sq. cm or 30 W/cm^2. Permissible dissipations are 30 to 110 W/sq. cm with flow rates of .25 to .50 gals./min/KW.

For water flow in small tubes (to 1" dia.)

$$V = 500 \left(\frac{h_f}{L} \right) \quad D_n^{2} \left(\frac{T + 10}{60} \right) \qquad \text{fps}$$

h_f & L in the same units,

water pressure is 30 psi,

length of tube is 1 1/4 ft.,

dia. of tube is .040 in.,

temp. T is $70^{\circ}F$

Substitution of these values in the above equation results in

$V = 59.3$ fps

$Q = VA = .23$ GPM

From this it is seen that with 30 psi of water pressure, that the cooling will be adequate. Since there are 25 grid tubes, the total flow will be 5.75 GPM.

The anode dissipation is 45KW and the area is approximately 796 sq. cm. The dissipation per unit area then is 56.5 watts/sq. cm which is well within the limits set forth above. The water flow required will be between 11 and 22 GPM, and must be turbulent. Calculations indicate that for the water jacket planned, 2 GPM would be adequate to produce turbulent flow. The inlet and outlet tubes to the anode water jacket are one inch diameter and five inches long.

For 30 psi at the inlet tube the flow through the tubes would be

$V = 46200$ fps or 252 GPM.

From this it is seen that there should not be any difficulty putting the required 11 to 22 GPM of cooling water through the water jacket for the stated pressure.

Envelope Experiments:

The tube was intended to have a ceramic envelope even though the contract does not specifically say so. Taking all of the design factors into account, a tube section was evolved as shown in Figure 21. This layout was predicated first upon the minimum emissive cathode area (200 sq. cm) required and an active length of 9 cm. These factors then decided the cathode diameter which ultimately decided the envelope diameter, viz. 9 inches. Examination of Figure 21 shows that the envelope cannot be made appreciably smaller in diameter. We found that obtaining ceramics this large did not present a major problem ($1\frac{1}{2}$ years ago) but obtaining metallized ceramics of 9 inches diameter was impossible. This meant that in addition to all of the problems of developing a structure, a furnace capable of metallizing must be obtained. About this time, announcements were made of a new alumino-silicate glass as well as a frit glass for lower temperature sealing (750 - 800°C). The glass frit after being sealed was capable of operation at 750°C which in general would be the upper temperature limit of a tube with a ceramic envelope. The alumino silicate glass supposedly would seal to molybdenum which must be done in a reducing atmosphere or a vacuum. Samples of the alumino silicate glass and frit glass were obtained and seals tried to various metals.

The alumino-silicate glass was tried with the frit and molybdenum. Since the molybdenum is easily oxidized, the heating was done in vacuum. The molybdenum disc was maintained at 775°C, for the prescribed hour by induction heating. The frit failed to seal to the alumino-silicate glass because of insufficient heat at that point although the frit was sealed to the molybdenum. The seal was very bubbly and looked as though it would leak. Sealing of the alumino-silicate glass directly to the molybdenum was then attempted. An adherent seal was obtained by inductively heating the molybdenum to 1300°C in vacuum. The glass cracked 1/8" above the seal due to high strain at that point.

We then tried sealing the alumino-silicate glass to Kovar, but the glass cracked in the same place because of what appeared to be a high strain caused by unequal heating of the glass.

Seals were then attempted with 7052, 7720, and aluminum oxide ceramic with the frit glass and Kovar. All but the 7052 cracked, showing definitely that the metal and glass or ceramic must match. The difference in thermal coefficients of expansion of Kovar and molybdenum is very slight in the region between 20 - 500 °C, but at the sealing temperature they are quite different. The expansion coefficient of the alumino-silicate glass must vary linearly with temperature the same as molybdenum. The

seal between 7052 and Kovar (Figure 22) was tested for vacuum tightness after being baked at 600°C and found to be satisfactory. The conclusions drawn from these tests are that the alumino-silicate glass does not even match molybdenum very well. The frit glass does wet the ceramic very well, but the metal required is either #52 alloy or one of the chrome-iron alloys. The former is desirable because it can be easily brazed, but the oxide films are not very adherent. The chrome iron has very adherent oxide films, but is very difficult to braze.

Another approach to the joining of ceramic and metal has been the use of the frit glass. Previous tests similar to that shown in Figure 22 resulted in cracked seals because of the mismatch between the Kovar and ceramic. By making the Kovar re-entrent as shown in Figure 23, we have been able to successfully join the Kovar and ceramic. This method looks simpler than metallizing the ceramics and would have been tried except time did not permit.

Seals between the alumino-silicate glass and Kovar similar to that shown in Figure 23 were made and indicated another degree of freedom.

When the large Litton furnace was finally set up, some test brazes were run and then some samples of ceramics were metallized with moly-manganese plus a small percentage of titanium hydride. The metallizing was good, but it almost ruined the furnace.

The trouble being that the furnace is lined with Inconel, melting point of about 1395°C; the firing temperature of the moly-manganese is 1325°C for one hour. The firing of the ceramic sample caused the Inconel liner to buckle and eventually it shorted out one filament. From this it appeared that we would be forced into using the alumino-silicate glass but trial seals in the Litton furnace indicated that considerably more work would have to be done before the alumino-silicate glass could be easily handled.

At this time it was fortunate that a low temperature (1100°C) technique developed by Raytheon was made available. This method employs a solution of the salts of a stable metal and glass former. The stable metal is provided by a water soluble molybdic acid salt and the glass former is provided by a water soluble salt of lithium. The solution is painted on the ceramic and then fired in hydrogen at 1100°C for three minutes. One very great advantage of this method is that the ceramics can be painted with the solution and after drying can be placed in the furnace with a copper washer between them and the metal disc to be brazed to them. The ceramics are metallized and brazed at the same time. This was tried with two pieces of aluminum oxide ceramic and found to yield excellent results.

The large ceramics were then coated and fired to metallize them. They were then brazed to the nickel flanges and found to be vacuum tight when tested with a helium leak detector. From this it would

appear that many of our problems were solved.

Assembly of the Breadboard Model:

The heater and cathode supports were brazed to the 5 inch diameter ceramic and nickel flanges with copper. On this subassembly the cathode and heater were assembled. The control and screen grids were then added along with the flanged ceramics (9" dia.) and this assembly brazed with a silver/copper eutectic. At this point some difficulty was experienced with holes in the brazes between the nickel flanges and the seal discs. The whole assembly was heated four times before all gaps were closed.

The large ceramic was next brazed to the anode/water jacket and just as the braze was completed, the ceramic cracked. It was maintained that the assembly was heated too rapidly in spite of the fact that two of the large ceramics were heated four times before with the identical schedule. They were heated three times to provide a good molybdenum coat and a fourth time to copper braze the flanges to the ceramics.

The braze between the second large ceramic and the anode/water jacket was attempted by bringing the temperature up very slowly. The temperature of the inside of the ceramic was monitored with a thermocouple and the temperature as a function of time is shown on Figure 24. The ceramic again cracked indicating that the cracking is due to the expansion of the nickel flange,

copper brazed to the ceramic and not because of thermal shock. The overall rate of temperature rise is 7°/min., whereas a piece of Nonex glass having the same thickness (1/2") can withstand a rate of rise of 5°/min. The ceramic is capable of withstanding a much greater rate of temperature rise, and does. During the metallizing process, the ceramic is heated to 1100°C in 70 minutes which is a rate of rise of almost 16°/min.

The five inch diameter ceramic located between the heater and cathode supports withstood repeated heating to 800°C. This ceramic has a 3/8 inch wall and has three-fourths the strength of the large ceramic (9" O.D., 1/2" wall), but is subjected to only five-ninths the stress. If the wall thickness of the large ceramic were increased to 3/4" the probability is that the ceramic would not crack when heated to 800°C (slightly above the melting point of the silver/copper eutectic).

The solution to the above basic difficulty is to thin out the edges of the seal discs and heli-arc weld the assemblies.

Since the parts on hand do not lend themselves to this method, and we do not have time to make the changes and fabricate new parts, the breadboard tube will be brazed together with hard solder.

Investigation of Gettering:

One of the provisions of the contract dealt with "The investigations into the feasibility of incorporating into the tube

an electrical gettering component which will continuously getter the tube with longer and more efficient tube life as the goal."

This section is most easily handled by adding a Vacuum pump to the tube. It is directly connected to the heater so that the power supply for the ion pump will not be very far from ground.

The ion pump not only provides continuous pumping action, but also provides a pressure reading.

Description of Tube:

The details of the tube and the methods of fabrication are most readily followed by reference to Figure 21.

All of the cold rolled steel parts are brazed together with Cubond which is a paste of powdered copper and an organic binder. The heater and cathode supports and the water jacket require no jigging. The control and screen grids require a base plate and mandrels to center the seal discs and grid tubes and maintain alignment. The stainless steel mandrels have 50 equally spaced slots, and determine the diameter of the control and screen grids, centering them within the seal discs and maintaining uniform pitch from one grid tube to the next. A grid is fabricated by painting both sides of a seal disc with Cubond and setting it in a grid tube ring on the stainless steel base plate as shown in Figure 25. A bead of Cubond is painted along the line between the grid tube ring and seal disc. The 25 preformed grid tubes are placed in the

holes in the grid tube ring and the appropriate mandrel is placed in the center. The grid tubes are then formed down onto the mandrel and bound in place with nickel wire (approximately 010" to 015" dia.). A bead of Cubond is then placed on the nickel grid tubes inside and outside the grid tube ring as shown in Figure 26. Spacers are placed between every other grid tube and the top seal disc put in place after having been painted with Cubond. A bead of Cubond is placed at the juncture of the top seal disc and grid tube ring as shown in Figure 27. The inside of the grid support ring is then painted with Cubond and placed on top of the grid tubes. A stainless steel ring is then placed on top of the top seal disc and the whole assembly heated in a hydrogen furnace until the Cubond melts and flows. The bottom support band is then brazed in place with gold/copper entectic. Assembly is then leak checked on a helium leak detector as shown in Figure 28. In this way the 50 brazes between the grid tubes and the grid tube ring as well as the brazes to the seal discs can be checked.

The large ceramics are all brazed to the flanges with copper. They are then helium leak checked as shown in Figure 29.

The heater and cathode supports are brazed to the flanges and the ceramics with copper, all at one time. They are leak checked in the same way as the grids, Figure 28.

After the heater and cathode are mounted on the support assembly, the grids are mounted thereon with a spacer between cathode and control grid as well as between control grid and screen. The joints between seal discs and flanges are then heli-arc welded. This assembly is then leak checked same as grids, Figure 28.

After the heater and cathode are mounted on the support assembly, the grids are mounted thereon with a spacer between cathode and control grid as well as between control grid and screen. The joints between seal discs and flanges are then heli-arc welded. This assembly is then leak checked same as grids, Figure 28.

The large diameter, long ceramic is assembled to the anode water jacket and leak checked similar to the method used for checking the ceramic to metal seals, Figure 29.

The final weld is made between the large ceramic flange and the screen grid seal disc.

The Vacion pump and tubulation were brazed to the tube prior to exhaust.

Static measurements in the negative grid region were taken during the exhaust procedure. The data was in substantial agreement with the calculated values.

Tube Characteristics:

The predicted characteristics are shown in Figure 30, which is a magnified replot of Figure 13. Heater voltage and current were very close to the calculated values.

Conclusions:

Based on the fabrication and processing techniques employed, it appears that the design is feasible. The ion-pumping is practical and desirable. Until full power test equipment is available, complete electrical data and performance cannot be evaluated.

Suggested Improvements and Future Work:

Some alterations are desirable. The manifolding of water into and out of the grids can be simplified by adding a single baffle between flanges of each grid.

By redesigning the sealing flanges and employing Kovar washers of the seal diameter, heli-arc welding of the joints will permit the tube to be disassembled readily if a defect occurs during operation.

Further suggestions for improvement and future work will have to await test results.

jg:mm

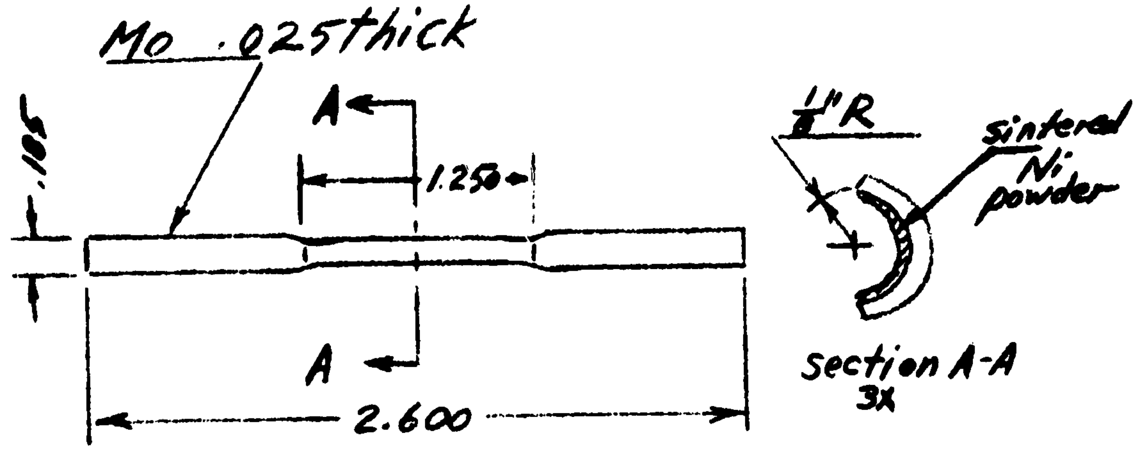

Matrix Cathode
for Test

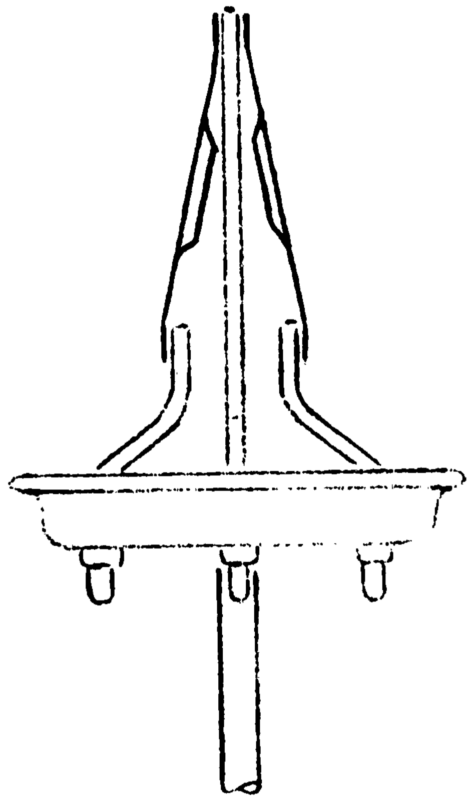

Cathode Test
Mount

XD32
Matrix Cathode

Fig. 1


Temperature
Saturation Curve
Matrix Cathode
Ep = 100 volts
Filament Current - Amps.
Plate Current - MA

Fig. 2

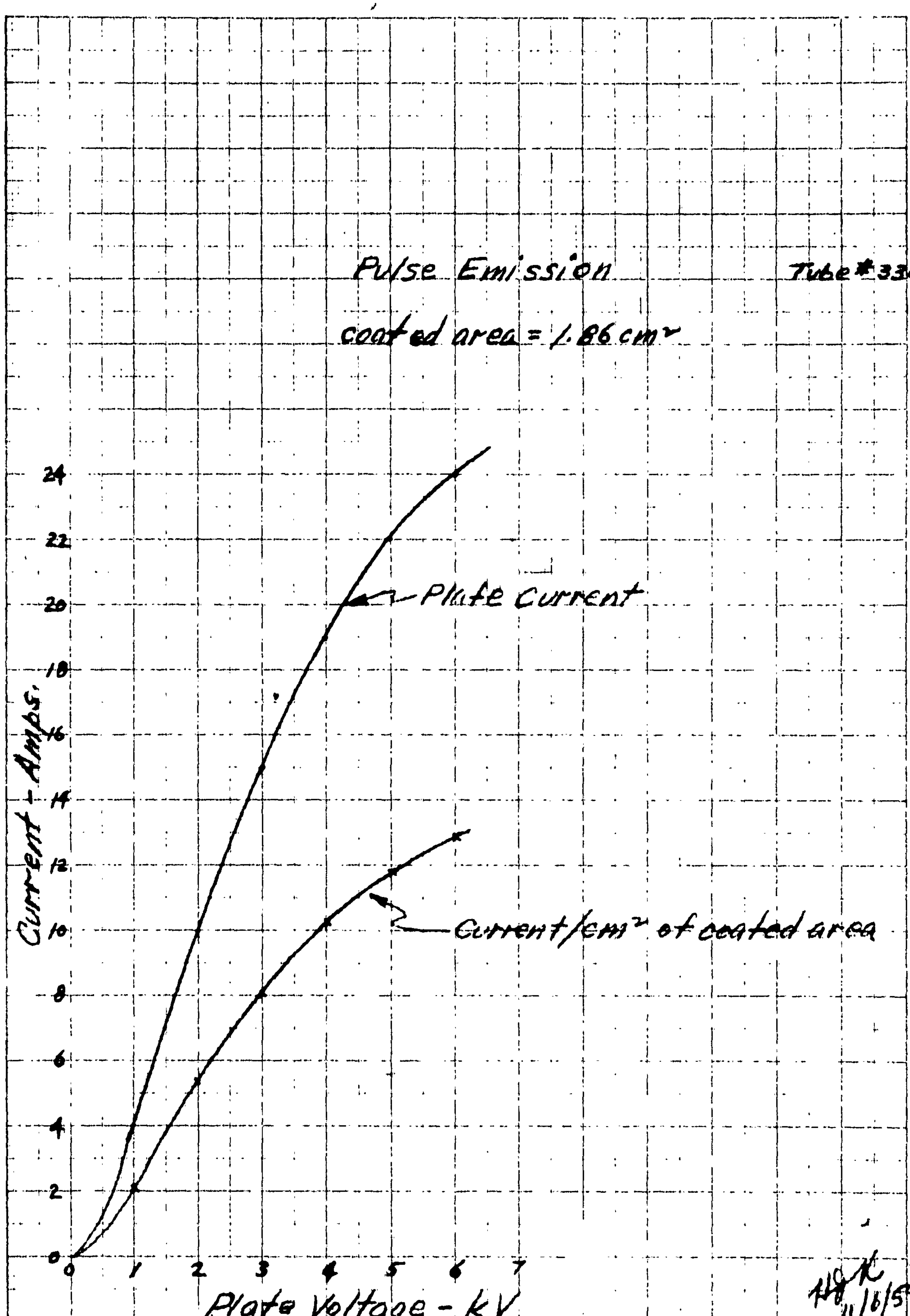
Pulse Emission
Tube # 336
coated area = 1.86 cm²
Plate current
Current/cm² of coated area
Current - Amps.
Plate Voltage - kV
0
2
4
6
8
10
12
14
16
18
20
22
24
0
1
2
3
4
5
6
7
11/6/59

Fig. 3

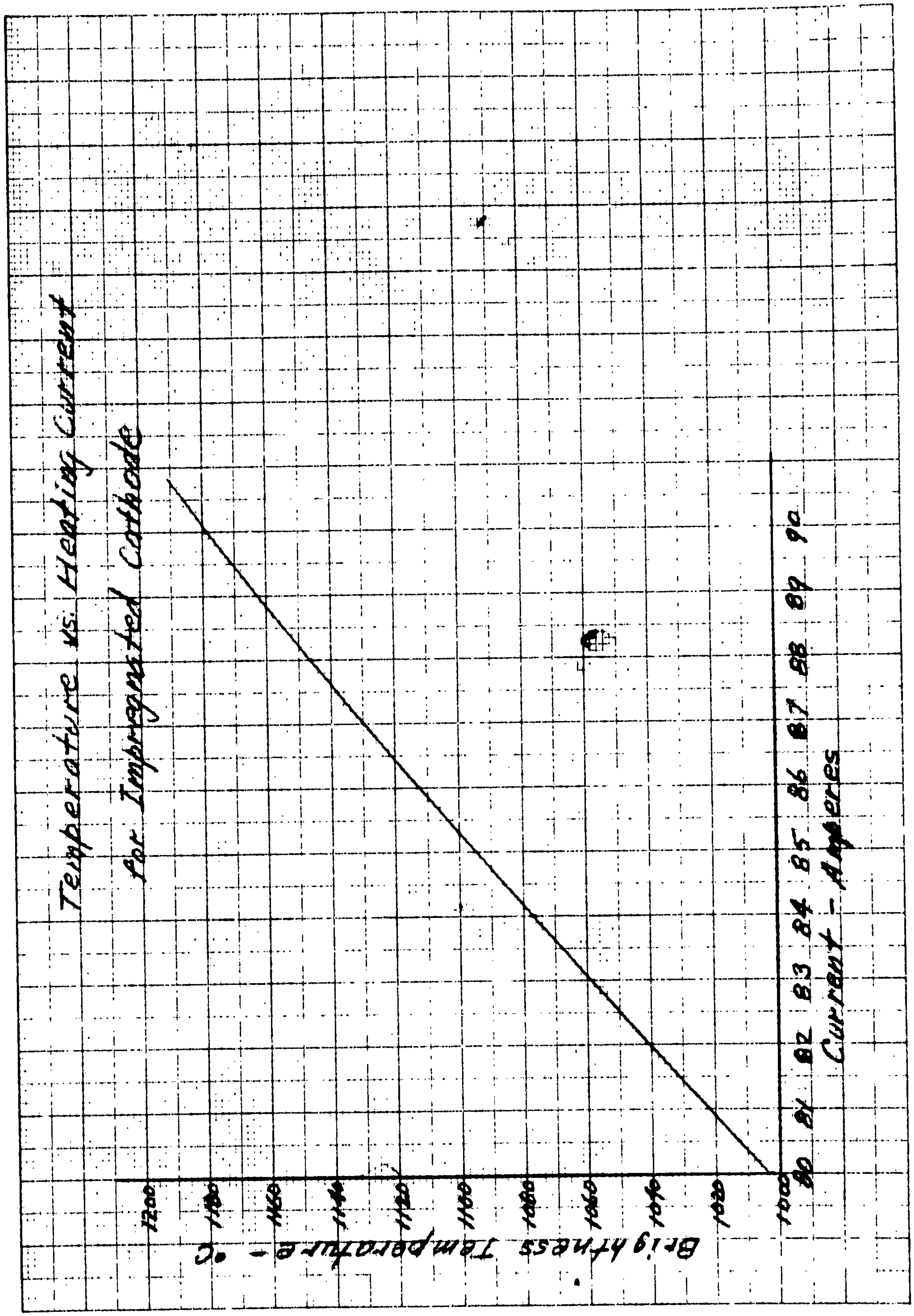
Temperature vs. Heating Current
for Impregnated Cathode
Brightness Temperature - °C
1000 1020 1040 1060 1080 1100 1120 1140 1160 1180 1200
Current - Amperes
80 81 82 83 84 85 86 87 88 89 90

Fig. 4

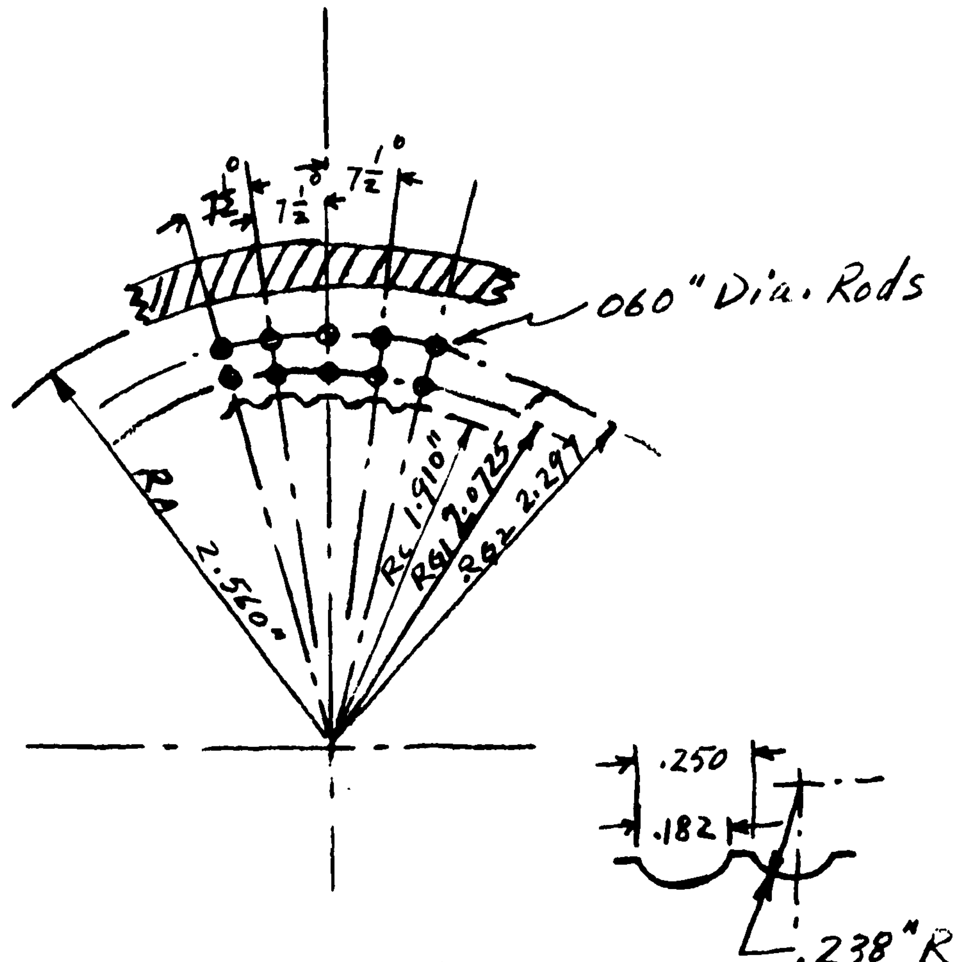

Tetrode With
Pierce Gun

Fig. 5

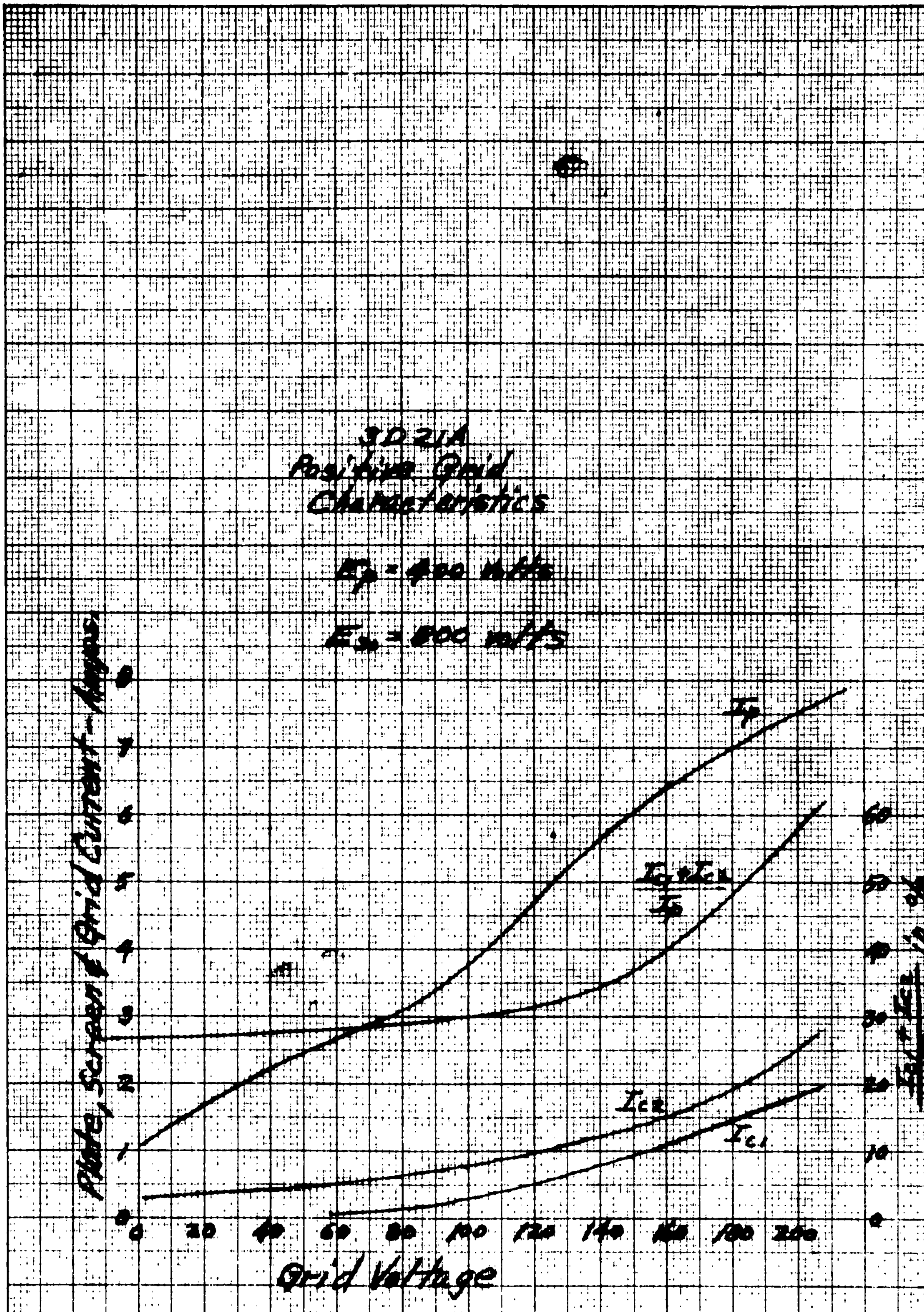
3D21A
Positive Grid
Characteristics
Ep = 400 volts
Es = 800 volts
Plate, Screen & Grid Current - Amperes
Grid Voltage
Ip
Ic2
Ic1
0
20
40
60
80
100
120
140
160
180
200
1
2
3
4
5
6
7
8
10
20
30
40
50
60

Fig 6

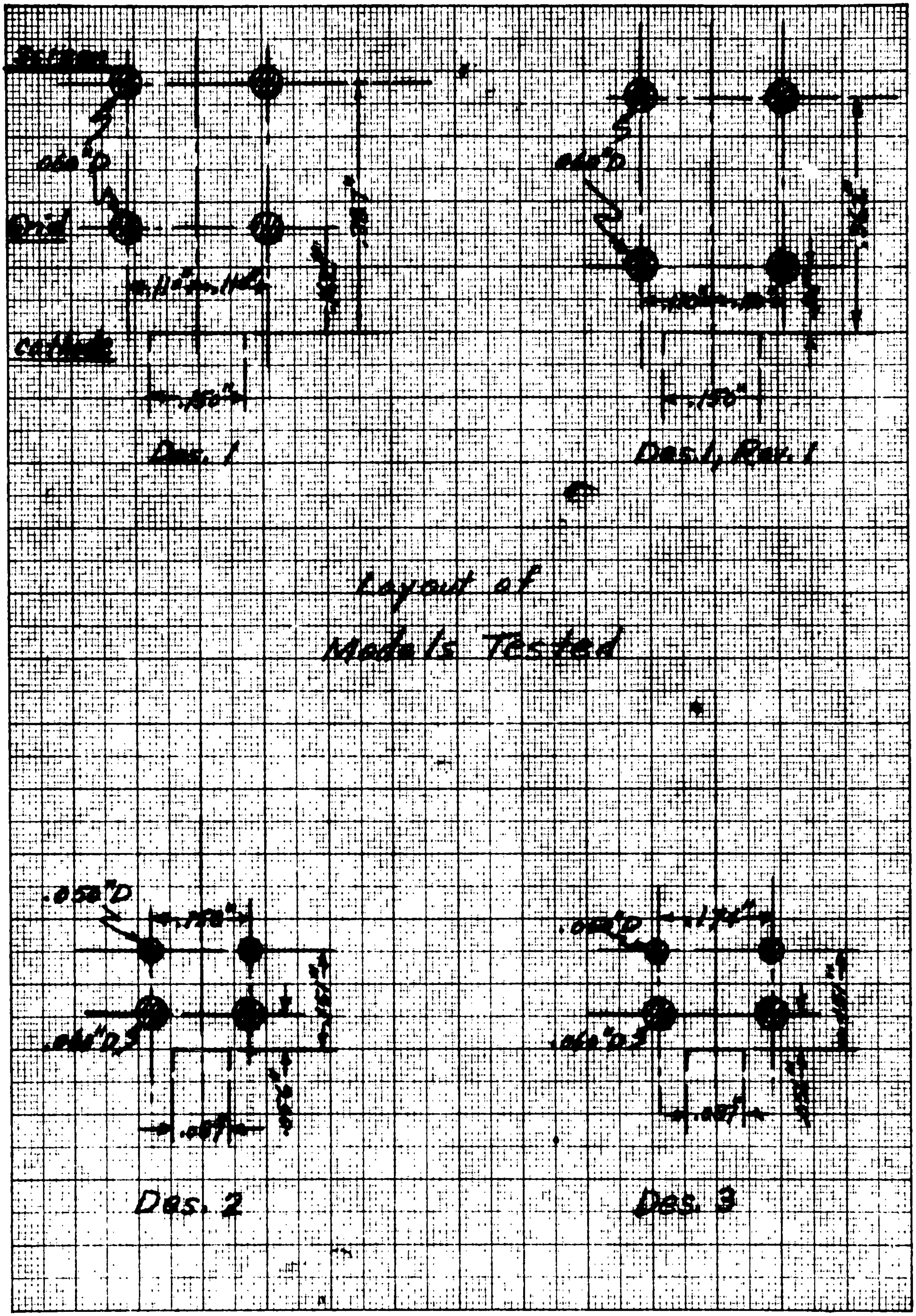
Grid
Cathode
Des. 1
Des. 1, Rev. 1
Layout of
Models Tested
.058"D
Des. 2
Des. 3

Fig. 8

KEUFFEL & ESSER CO., N. Y. NO. 359-11
10 X 10 to the ½ inch. 5th lines accented.
MADE IN U. S. A.

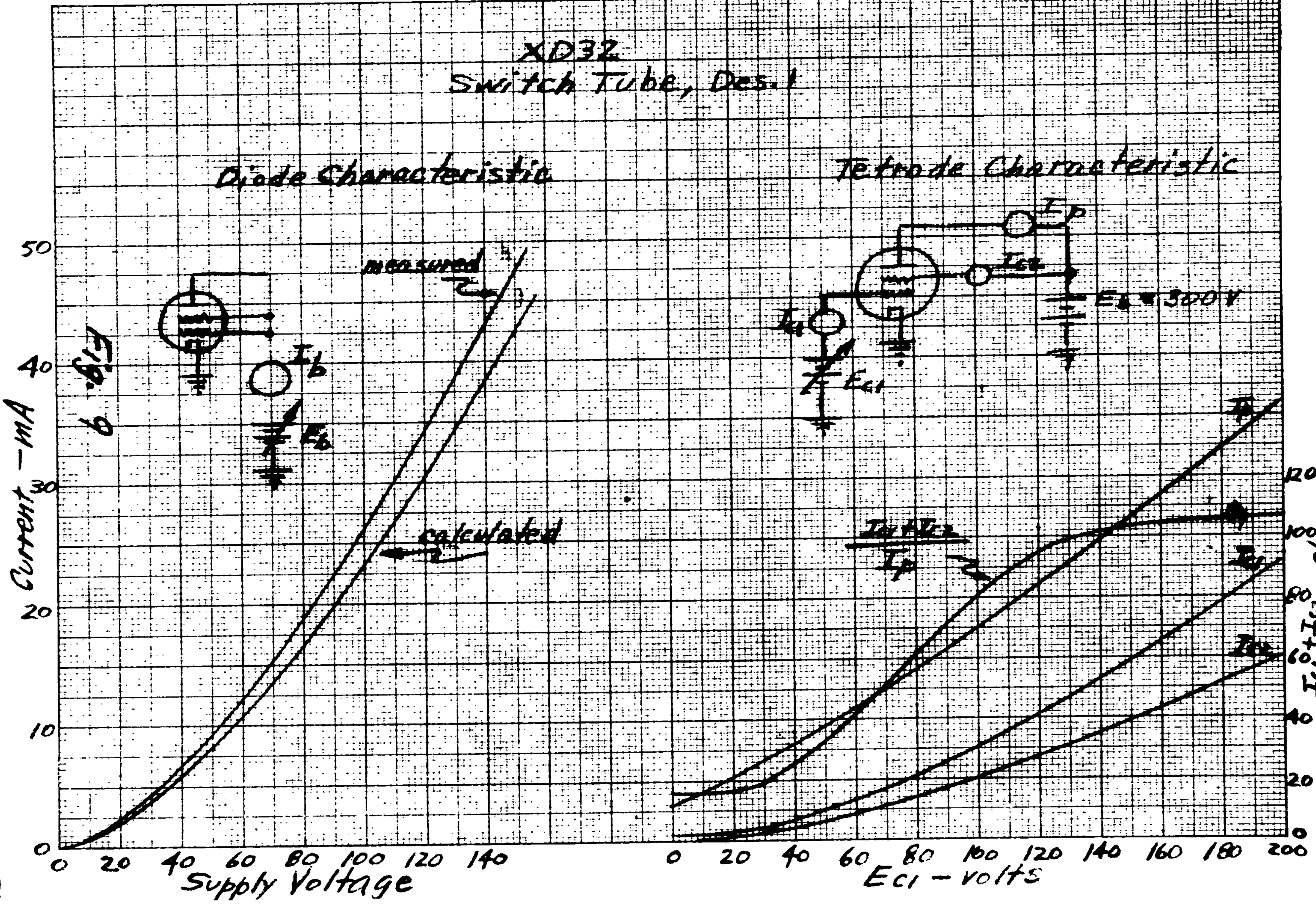

Fig. 9

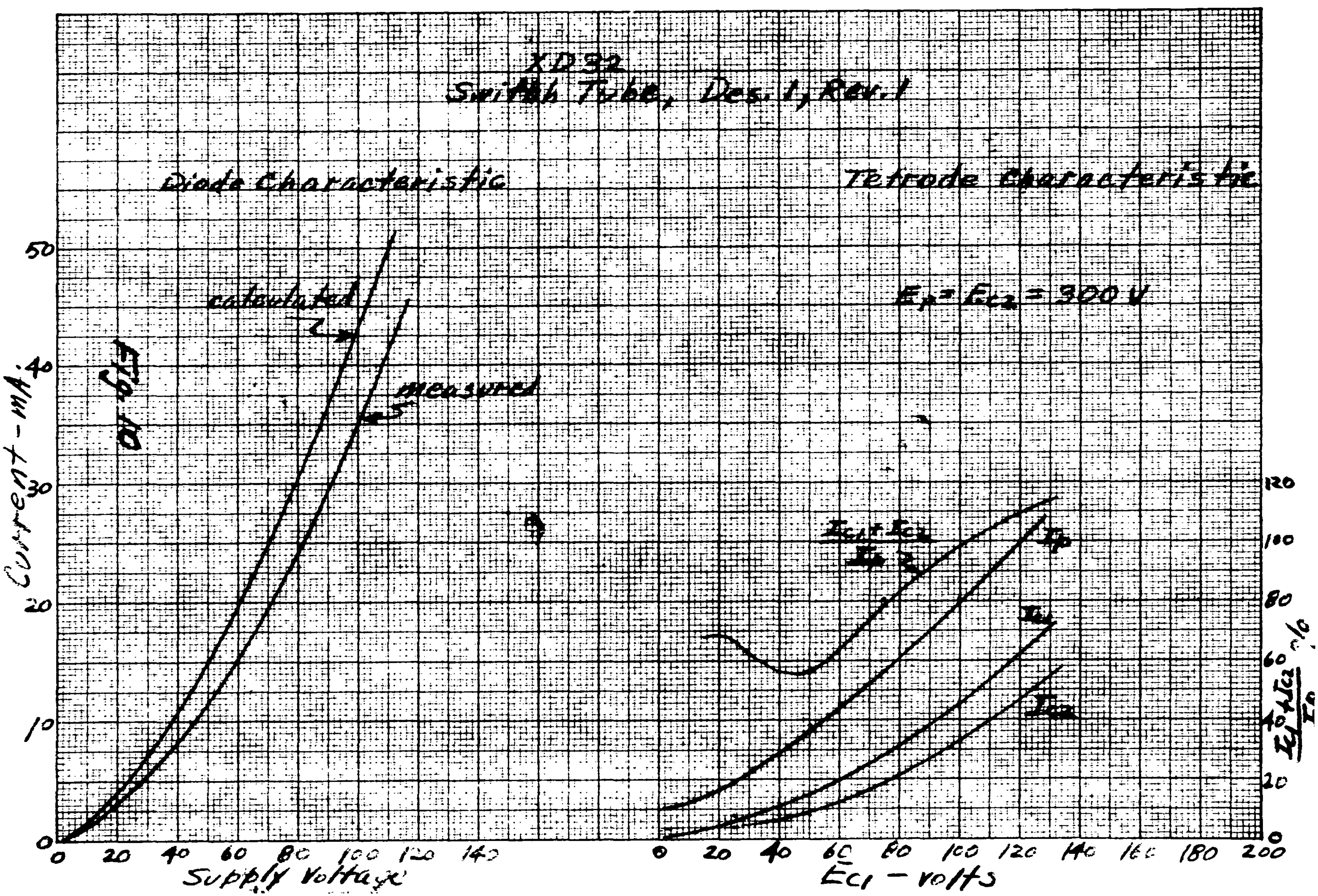
XD32
Switch Tube, Des. 1, Rev. 1
Diode Characteristic
Tetrode Characteristic
calculated
measured
$E_p = E_{c2} = 300$ V
$\frac{I_{c1} + I_{c2}}{I_p}$
I_p
I_{c1}
I_{c2}
Current - mA.
Supply Voltage
E_{c1} - volts
$\frac{I_{c1} + I_{c2}}{I_p}$ %
0
10
20
30
40
50
0
20
40
60
80
100
120
140
0
20
40
60
80
100
120
140
160
180
200
0
20
40
60
80
100
120

Fig. 10

KEUFFEL & ESSER CO., N. Y. NO. 359-11
10 x 10 to the ½ inch, 5th lines accented
MADE IN U.S.A.

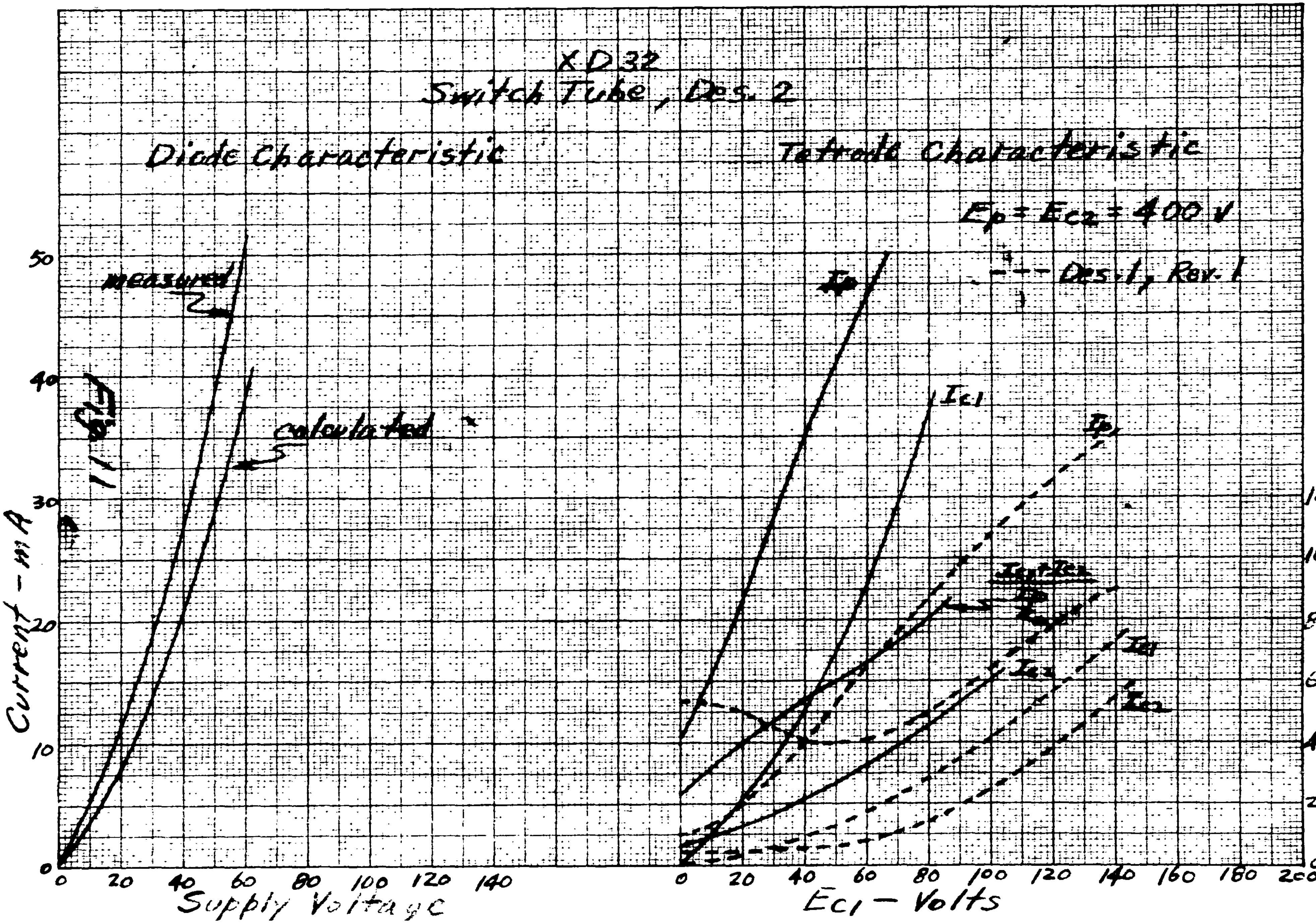

Fig. 11

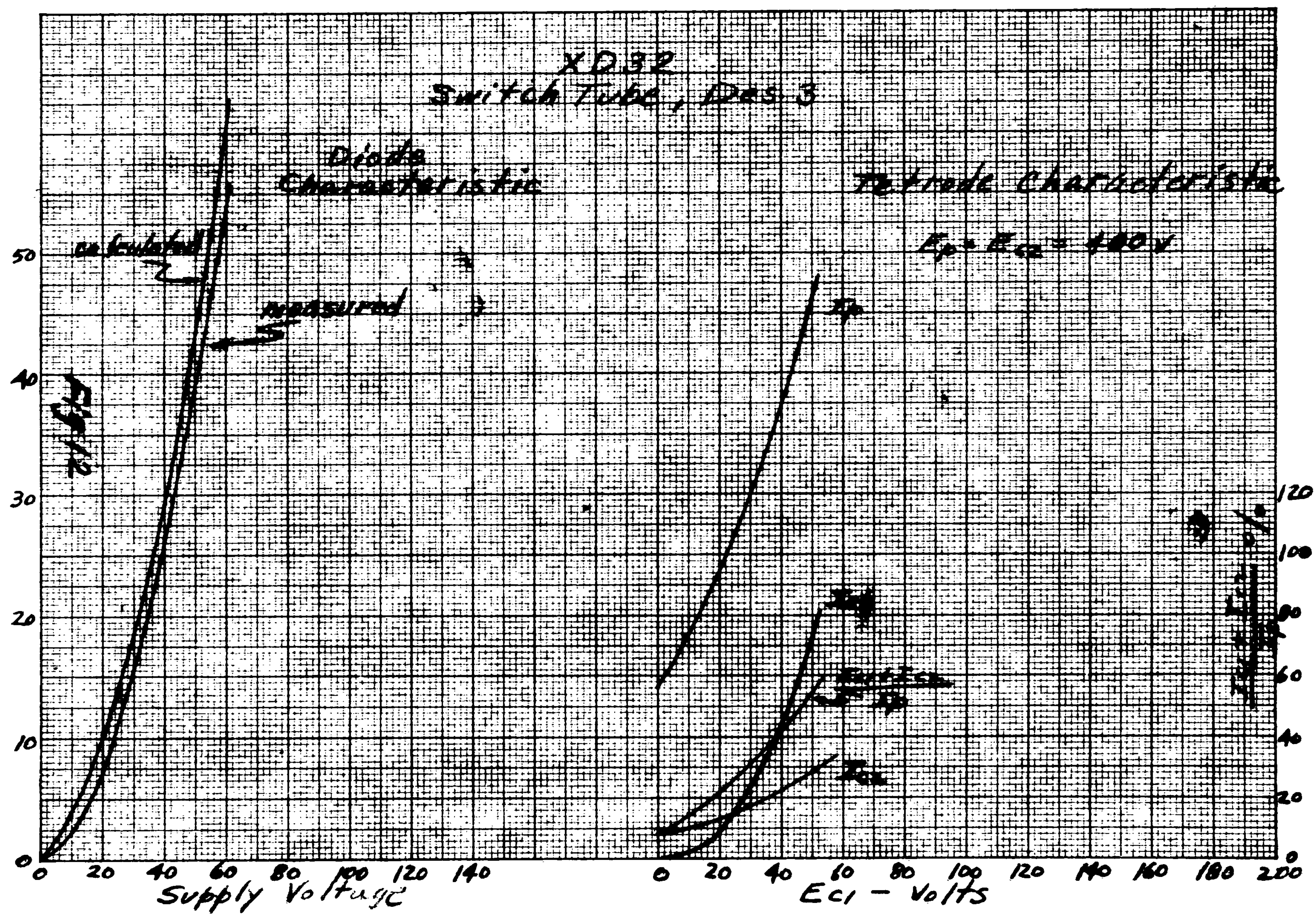
XD32
Switch Tube, Des. 3
Diode Characteristic
calculated
measured
Tetrode Characteristic
$E_p = E_{c2} = 180V$
I_p
I_{c2}
I_{c1}
0
10
20
30
40
50
0
20
40
60
80
100
120
140
Supply Voltage
0
20
40
60
80
100
120
140
160
180
200
E_{c1} - Volts
0
20
40
60
80
100
120
Fig 12

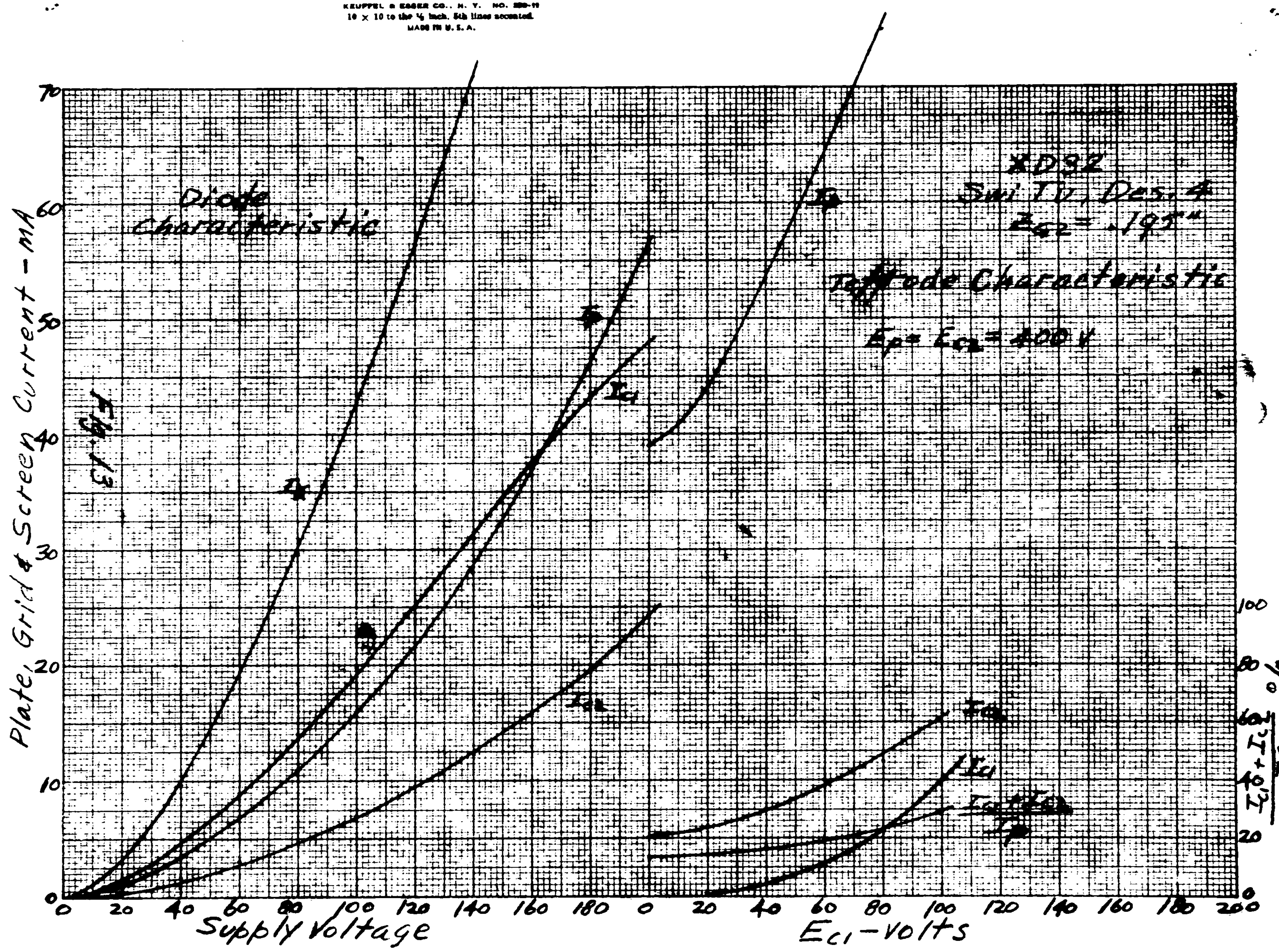
XD32
Swi Tv. Des. 4
Z_{G2} = .195"
Tetrode Characteristic
$E_p = E_{c2} = 400$ V
Diode Characteristic
Fig. 13
Plate, Grid & Screen Current - MA
Supply Voltage
E_{c1} - volts
% $\frac{I_{c1}+I_{c2}}{I_p}$
I_b
I_p
I_{c1}
I_{c2}

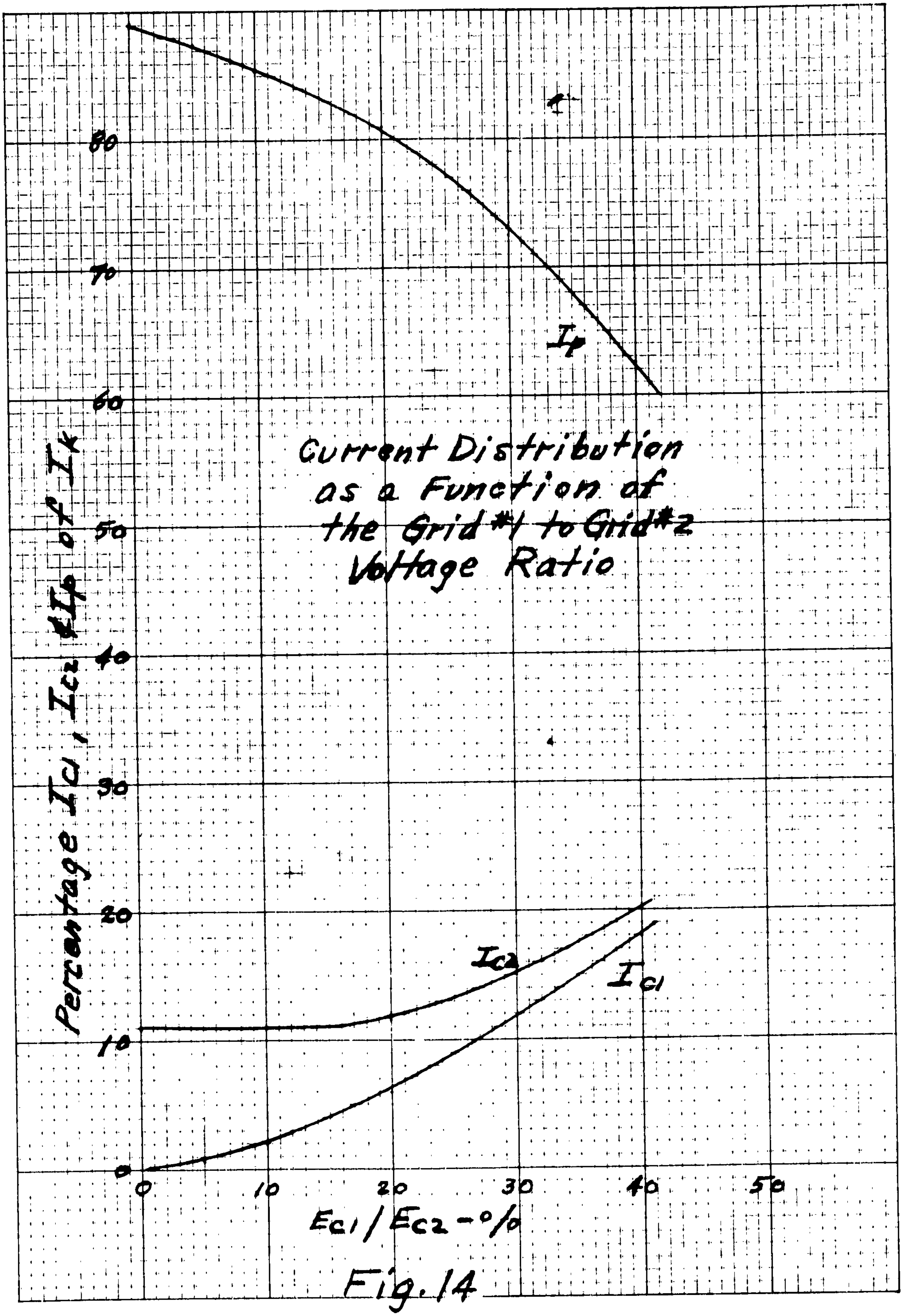

Current Distribution
as a Function of
the Grid #1 to Grid #2
Voltage Ratio
Percentage I_{c1}, I_{c2} & I_p of I_k
I_p
I_{c2}
I_{c1}
E_{c1}/E_{c2} - %
0
10
20
30
40
50
60
70
80

Fig. 14

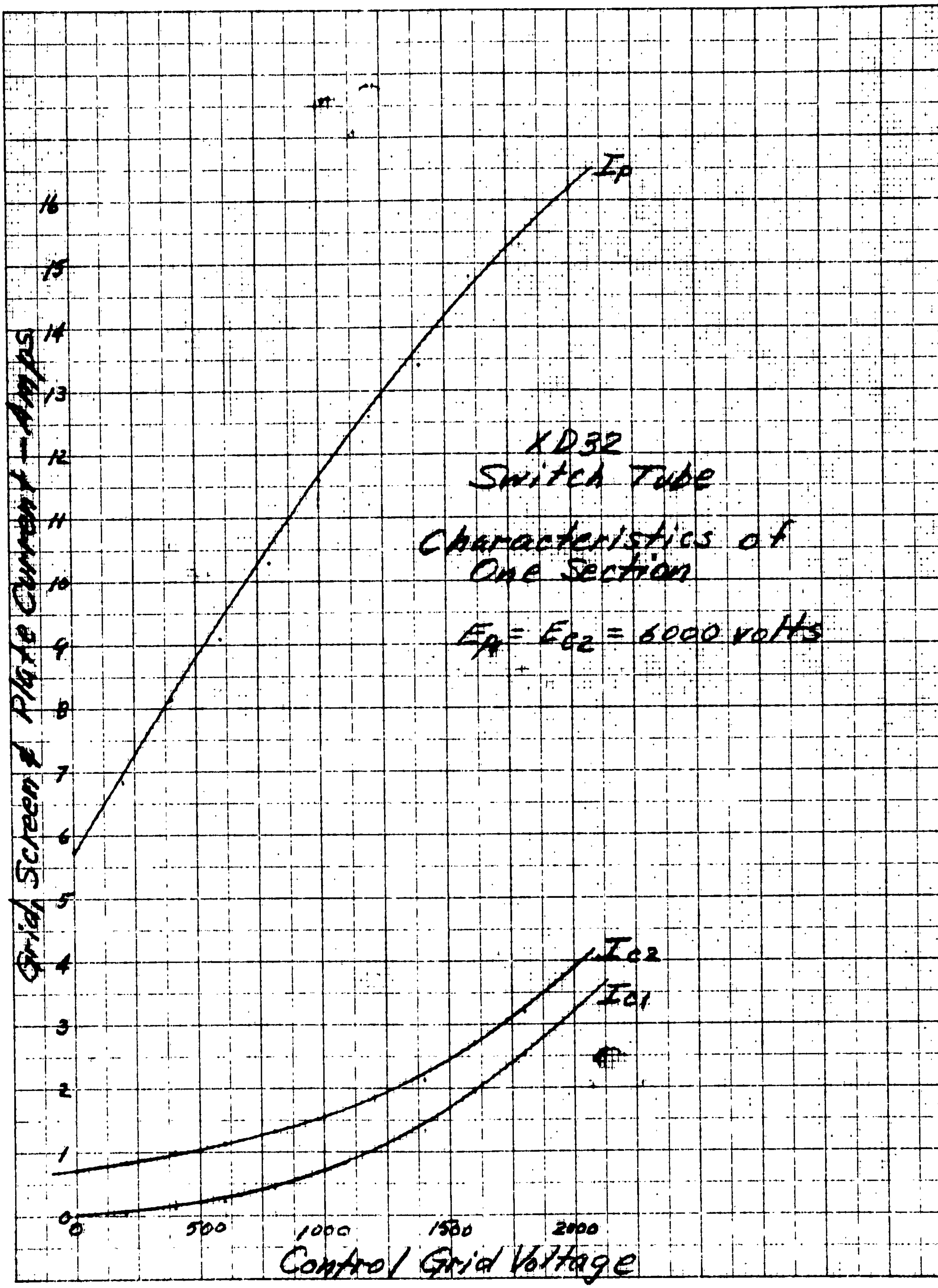
Ip
16
15
14
13
12
11
10
9
8
7
6
5
4
3
2
1
0
Grid, Screen & Plate Current - Amps
XD32
Switch Tube
Characteristics of
One Section
$E_A = E_{c2} = 6000$ volts
I_{c2}
I_{c1}
0
500
1000
1500
2000
Control Grid Voltage

Fig. 15

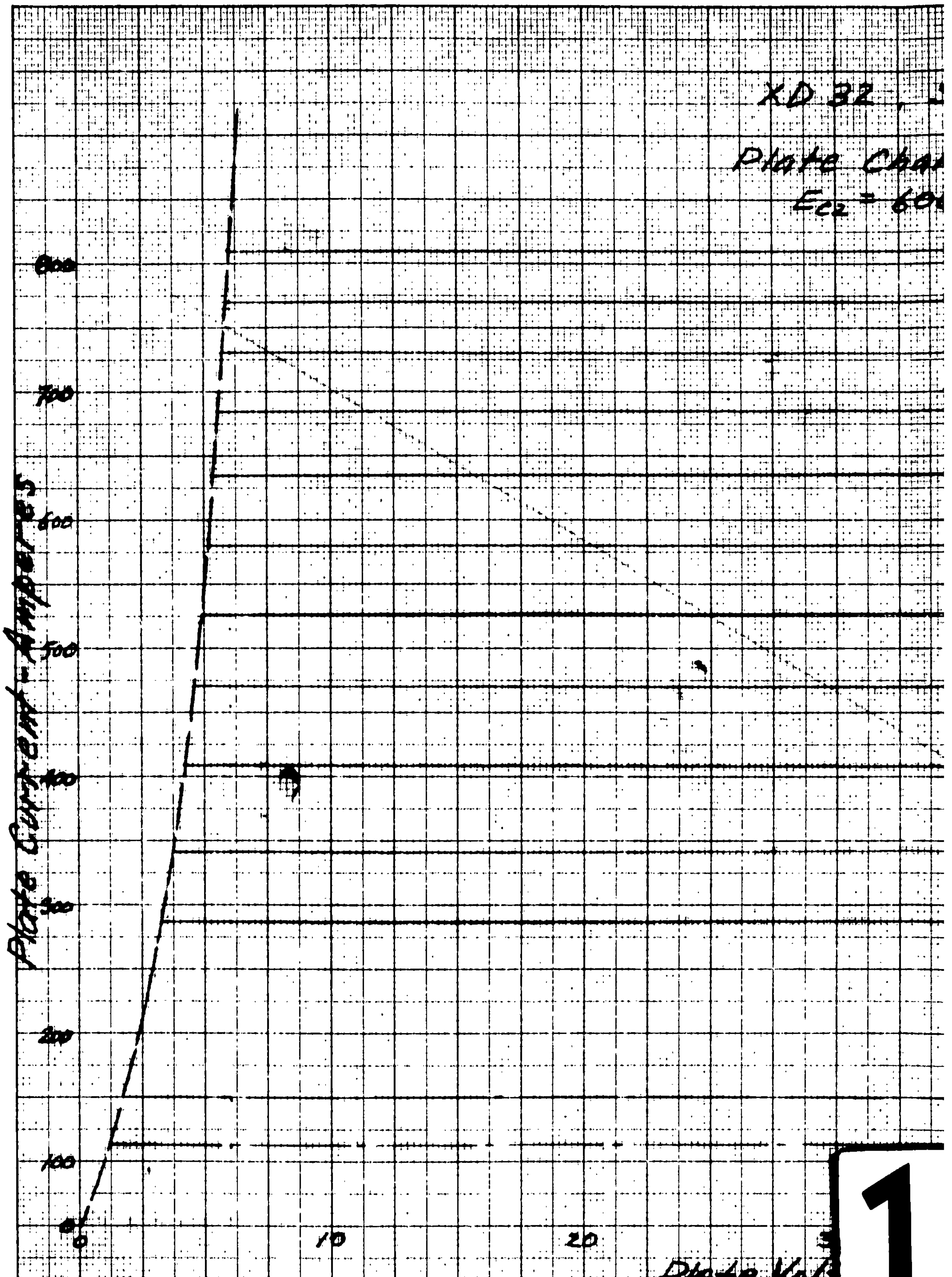
XD 32 ,
Plate Cha
E_{c2} = 60
Plate Current - Amperes
800
700
600
500
400
300
200
100
0
0
10
20
Plate Vol

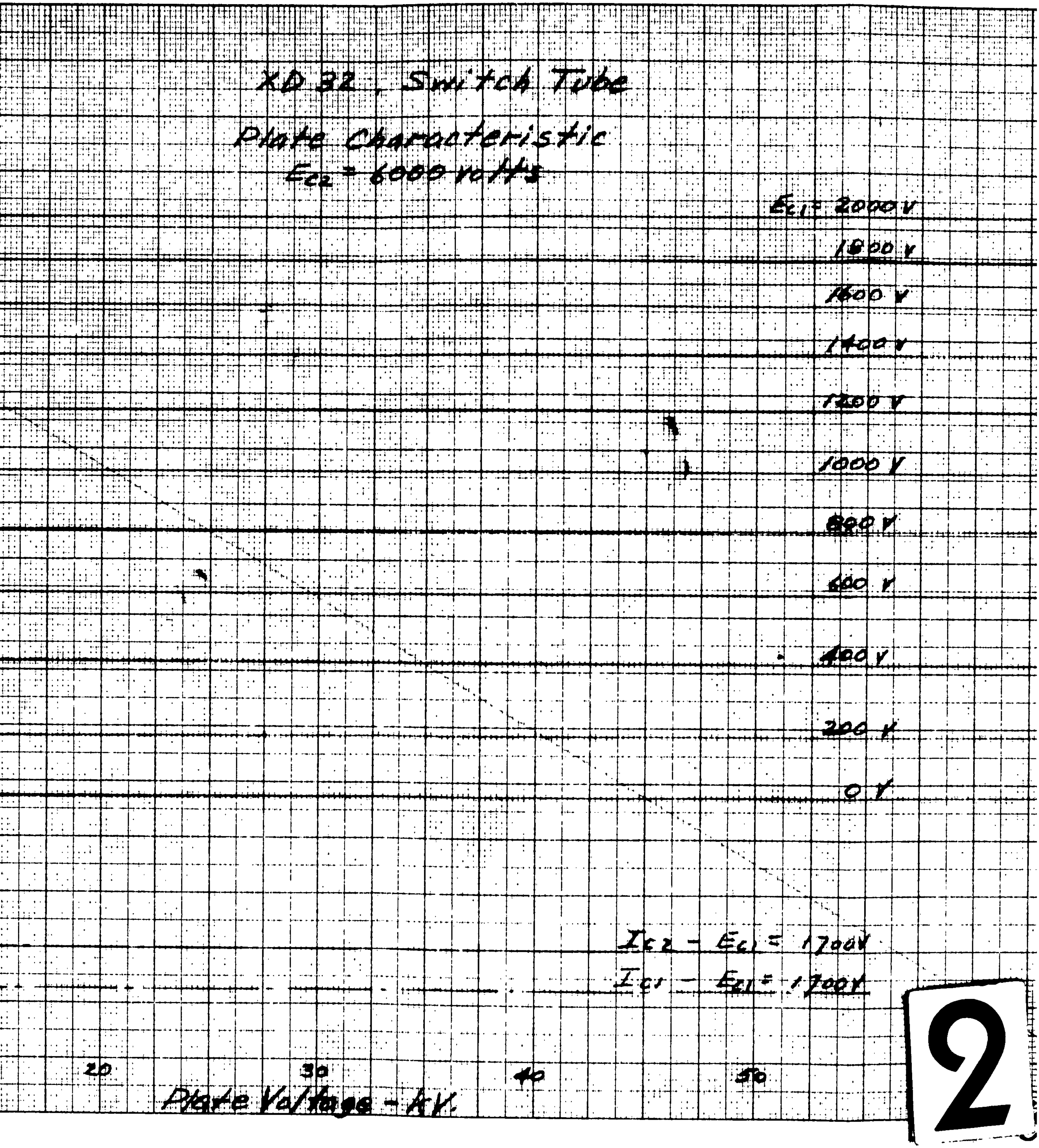
XD 32, Switch Tube
Plate Characteristic
Ec2 = 6000 volts
Ec1 = 2000 V
1800 V
1600 V
1400 V
1200 V
1000 V
800 V
600 V
400 V
200 V
0 V
Ic2 – Ec1 = 1700 V
Ic1 – Ec1 = 1700 V
20
30
40
50
Plate Voltage - kV.
2

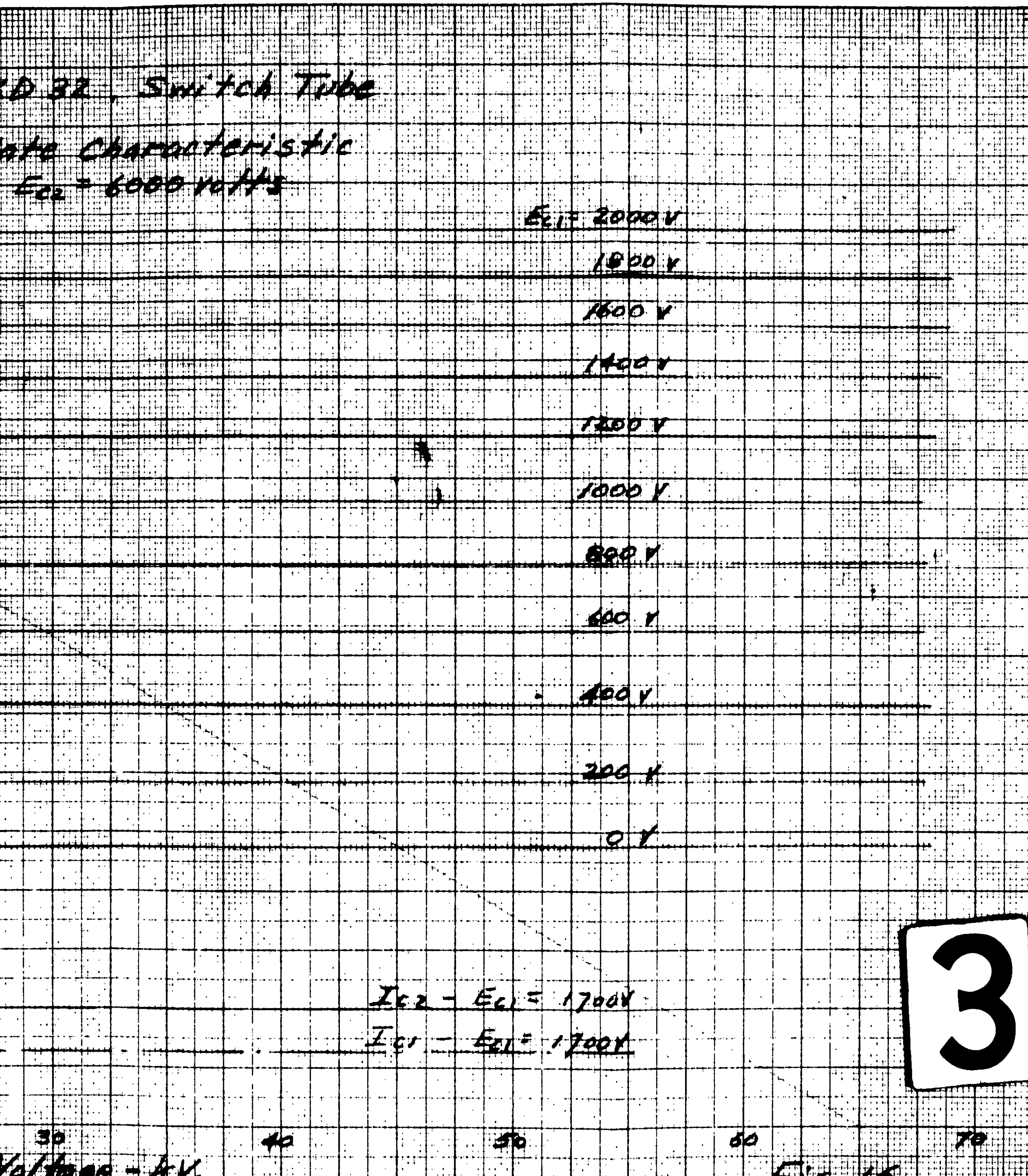
D 32 , Switch Tube
ate Characteristic
E_{c2} = 6000 volts
E_{c1} = 2000 V
1800 V
1600 V
1400 V
1200 V
1000 V
800 V
600 V
400 V
200 V
0 V
I_{c2} — E_{c1} = 1700 V
I_{c1} — E_{c1} = 1700 V
30
40
50
60
70
Voltage - KV.
3

Fig. 16

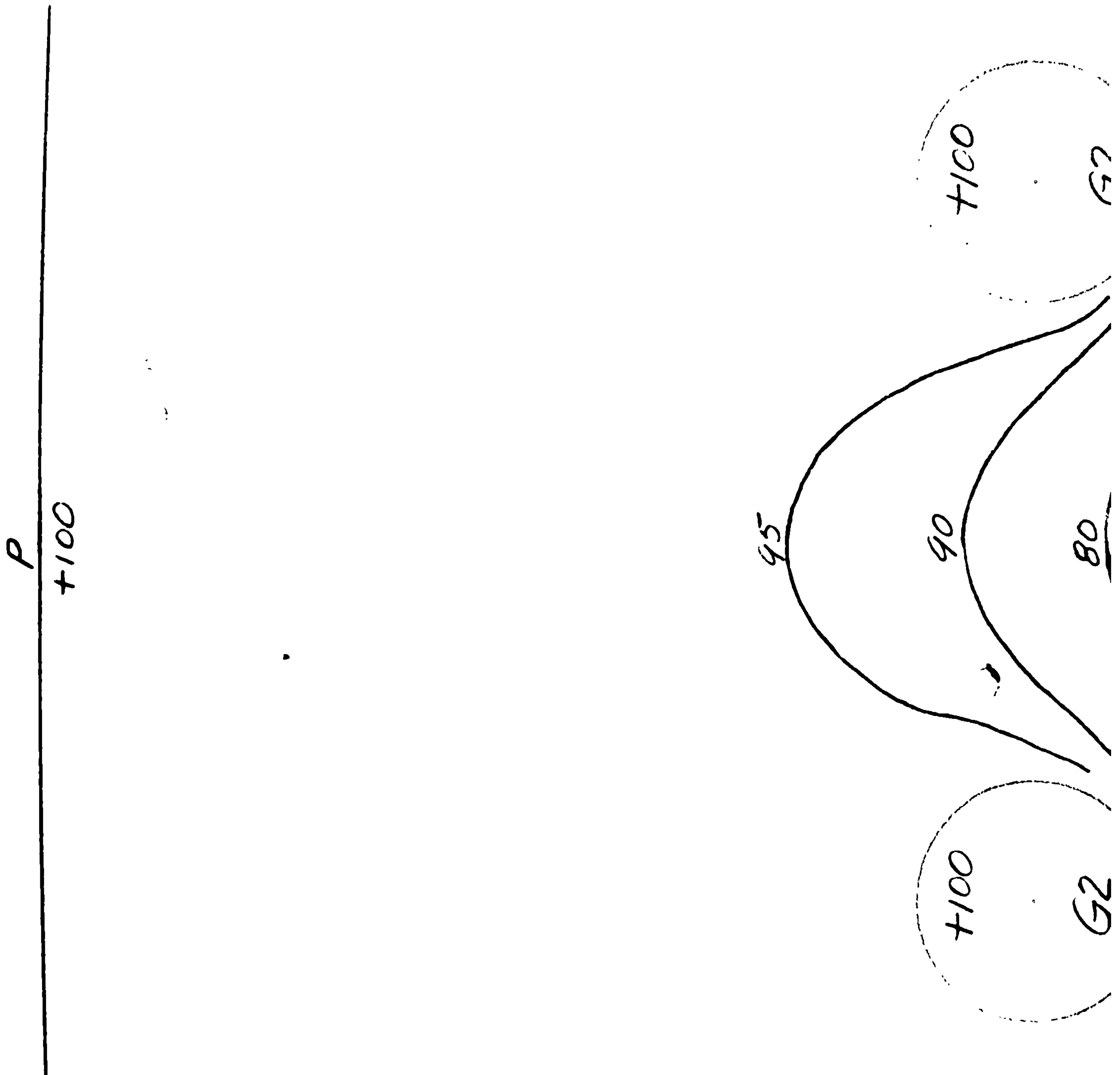

1

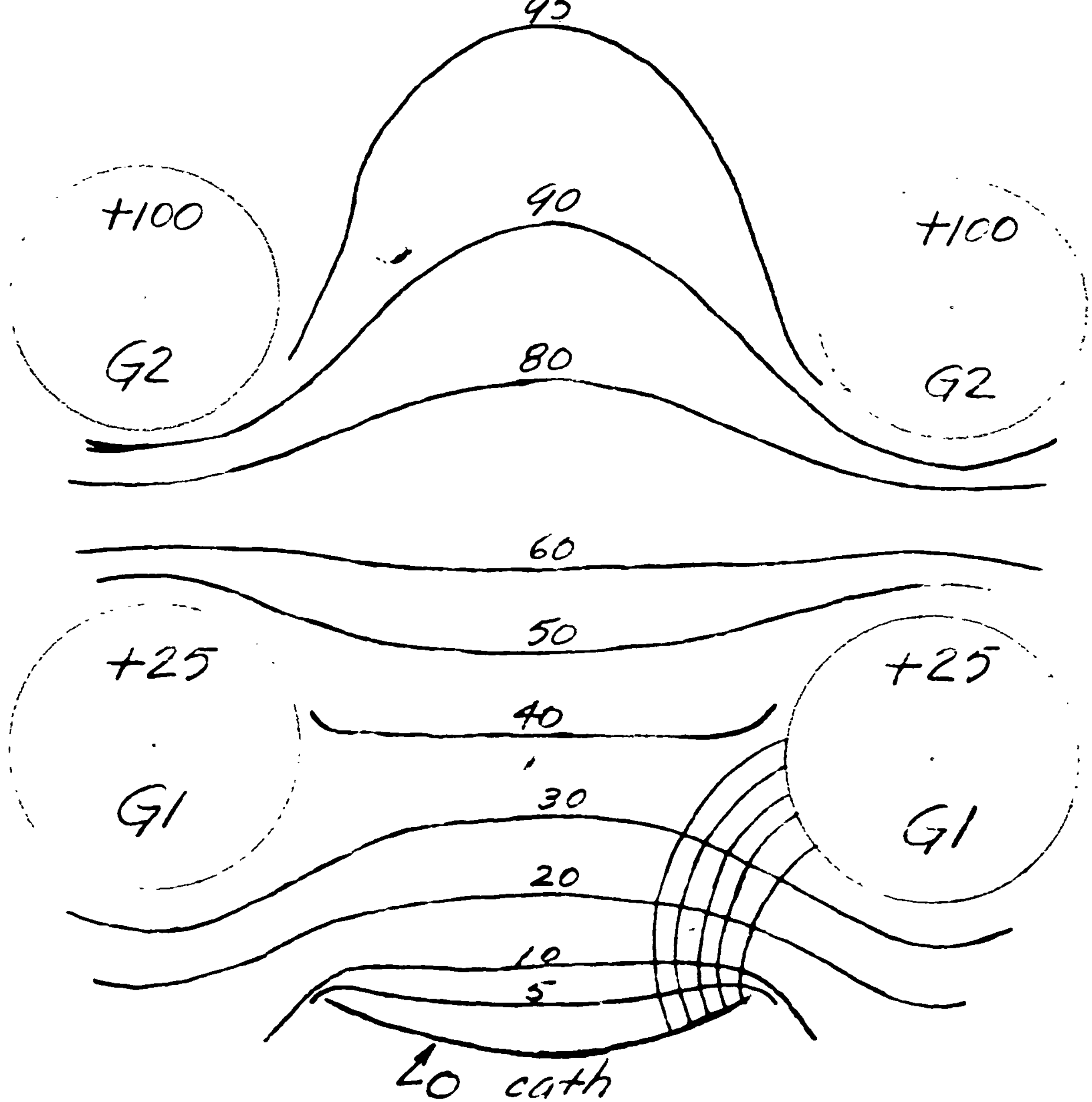

2

Des. 3

Fig. 17

Scale: 30X

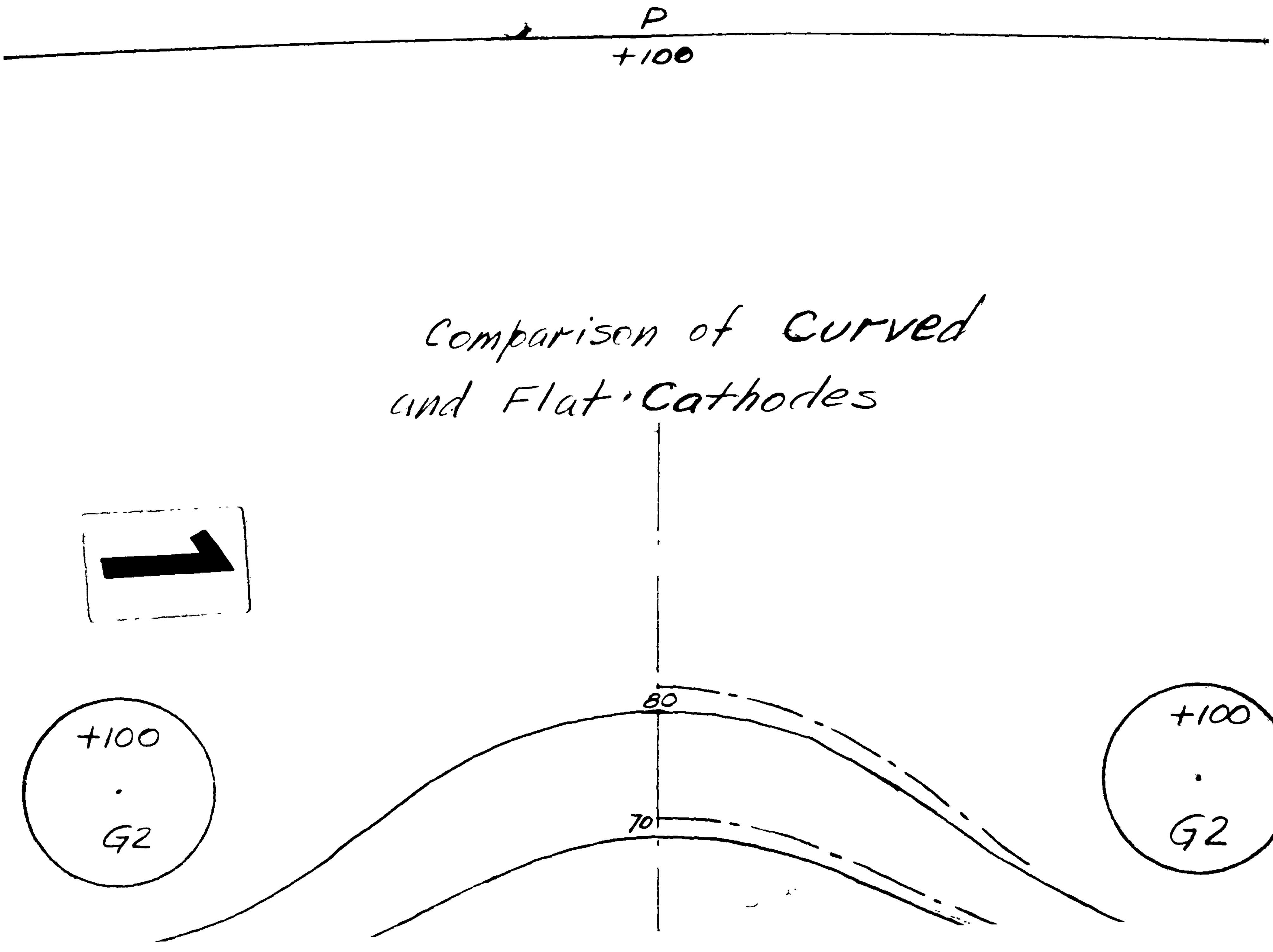

Comparison of Curved and Flat Cathodes

1

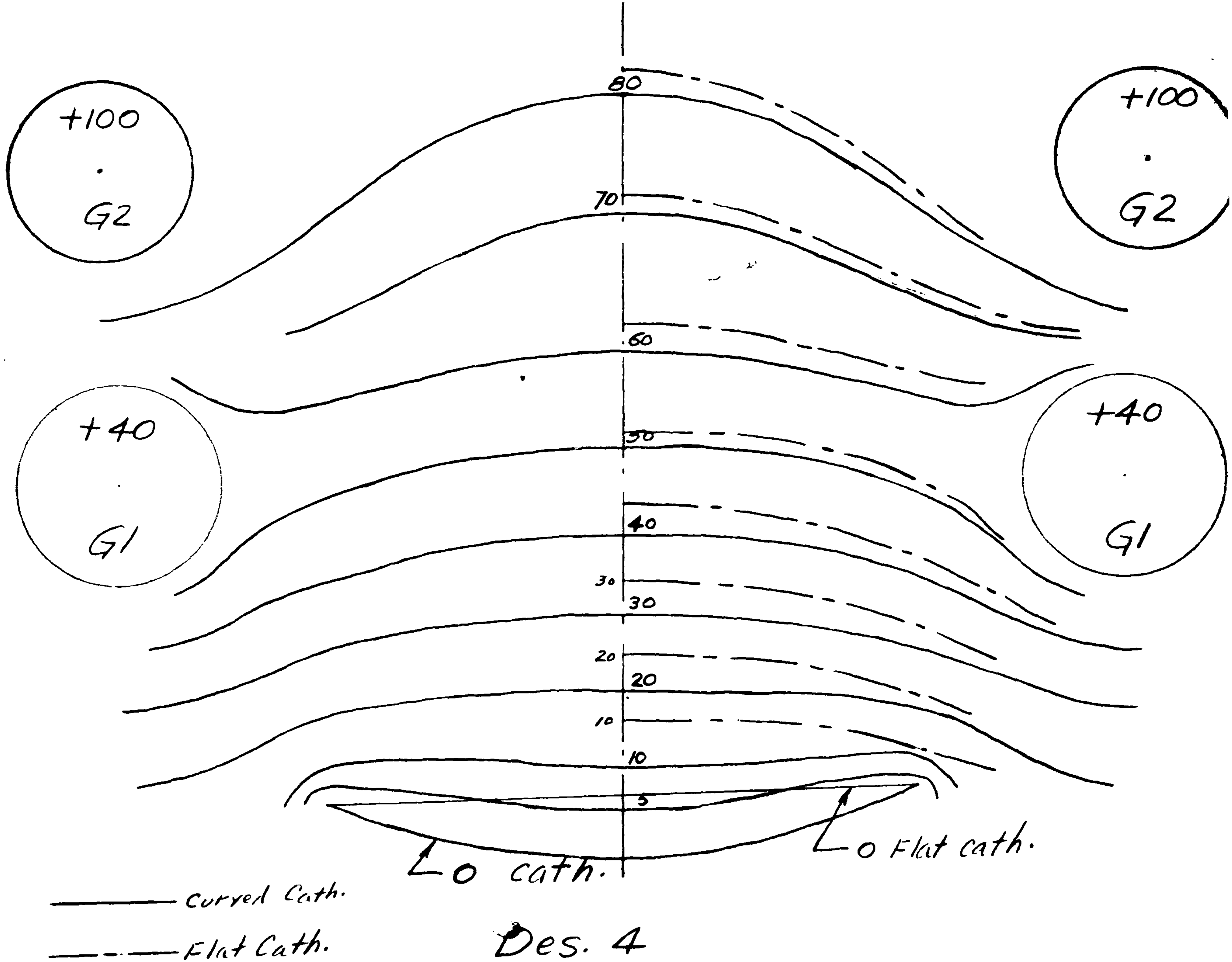

Des. 4

Fig. 18

Scale: 30X

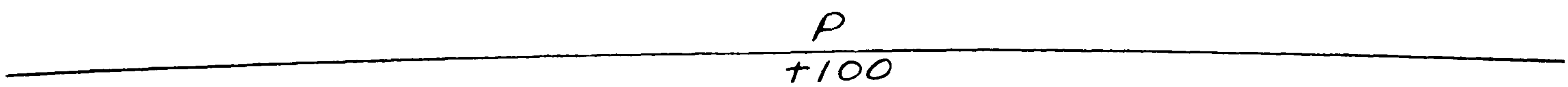

Comparison of Round
and Flat Screen Rods

1

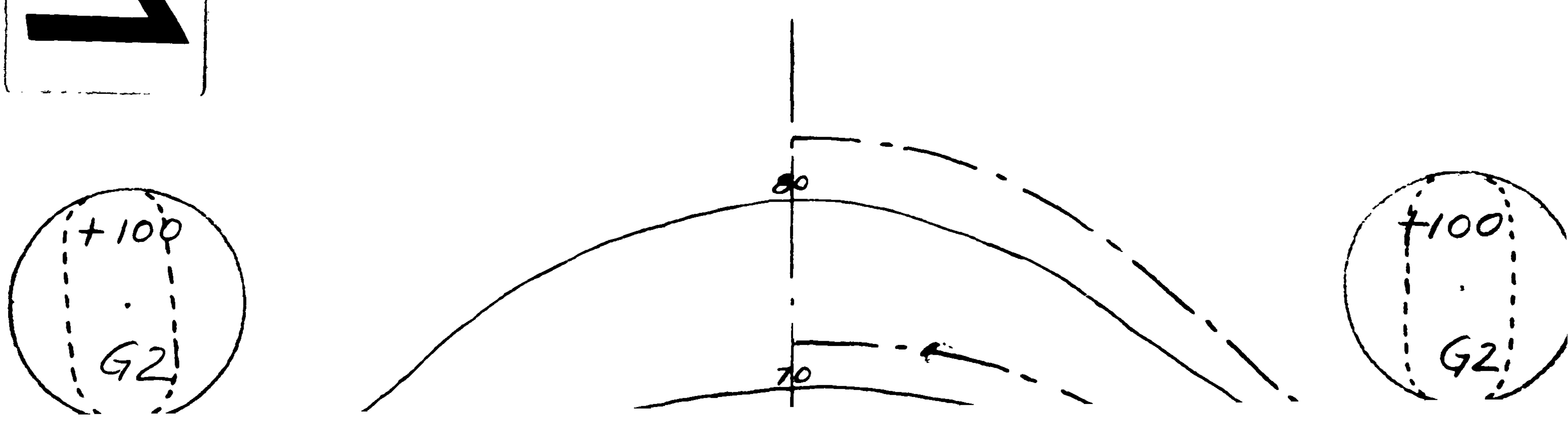

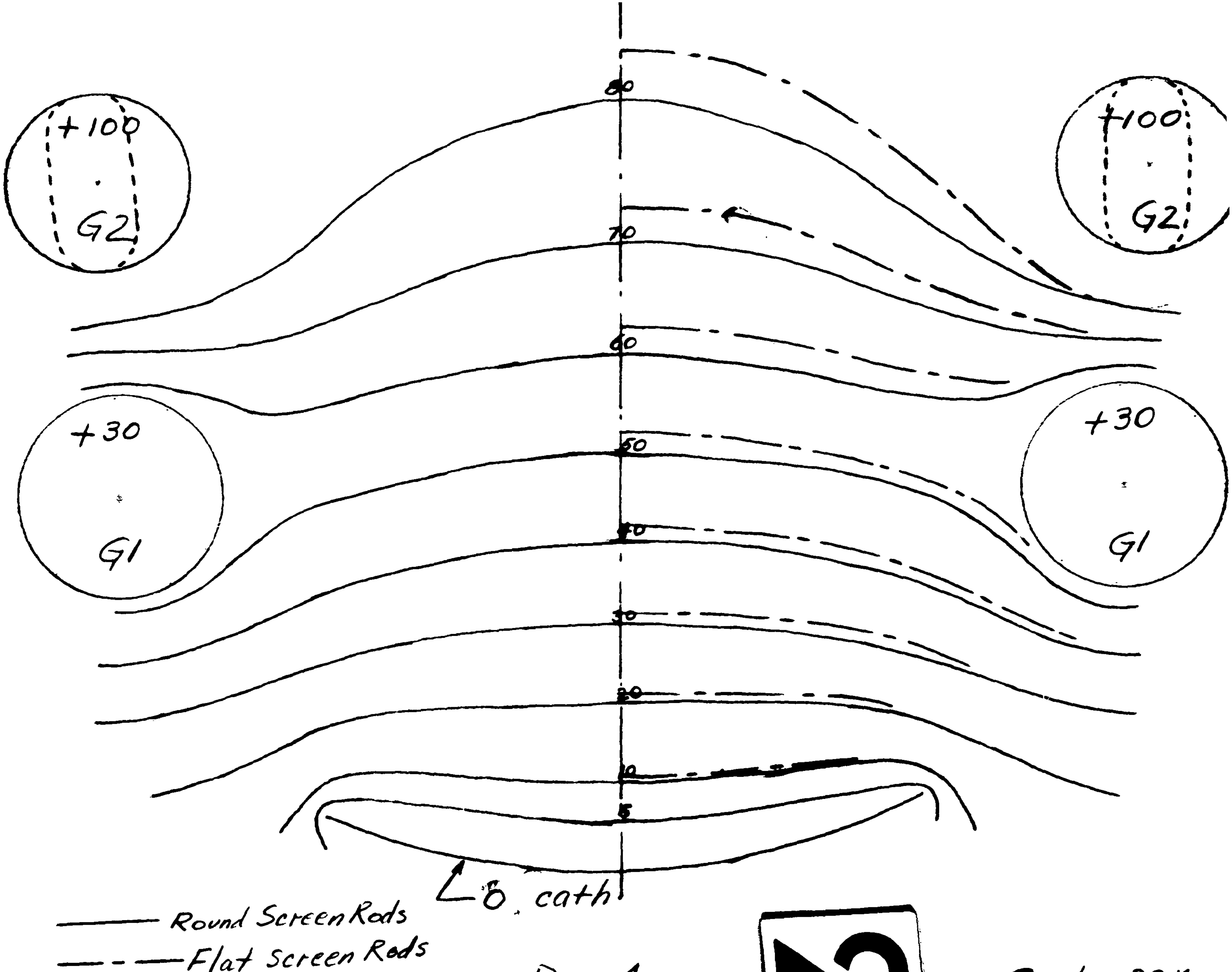

Des. 4

Scale: 30x

2

Fig. 19

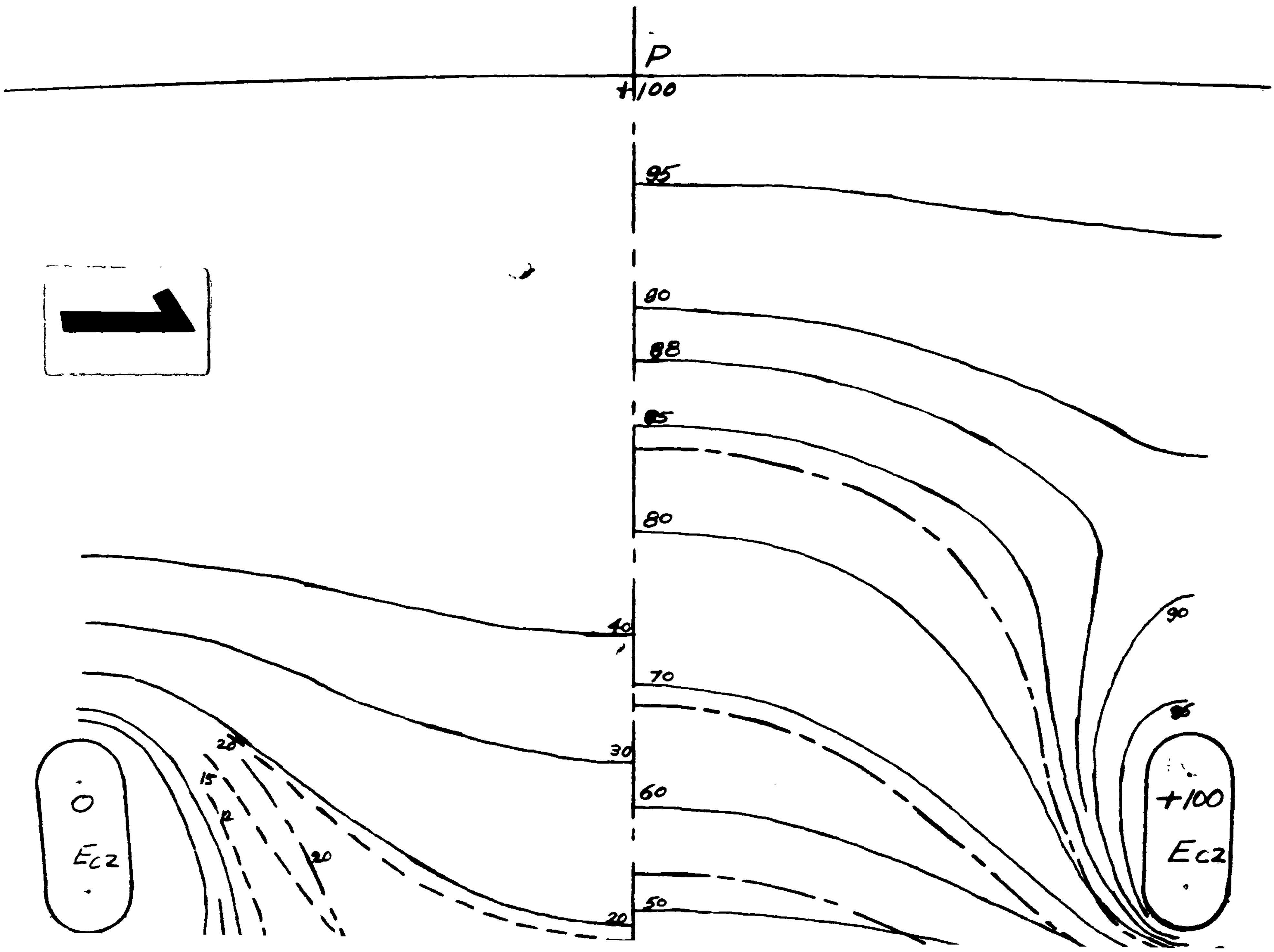

P
+100
95
90
88
85
80
70
60
50
40
30
20
90
95
+100
Ec2
O
Ec2
20
15
12
20
1

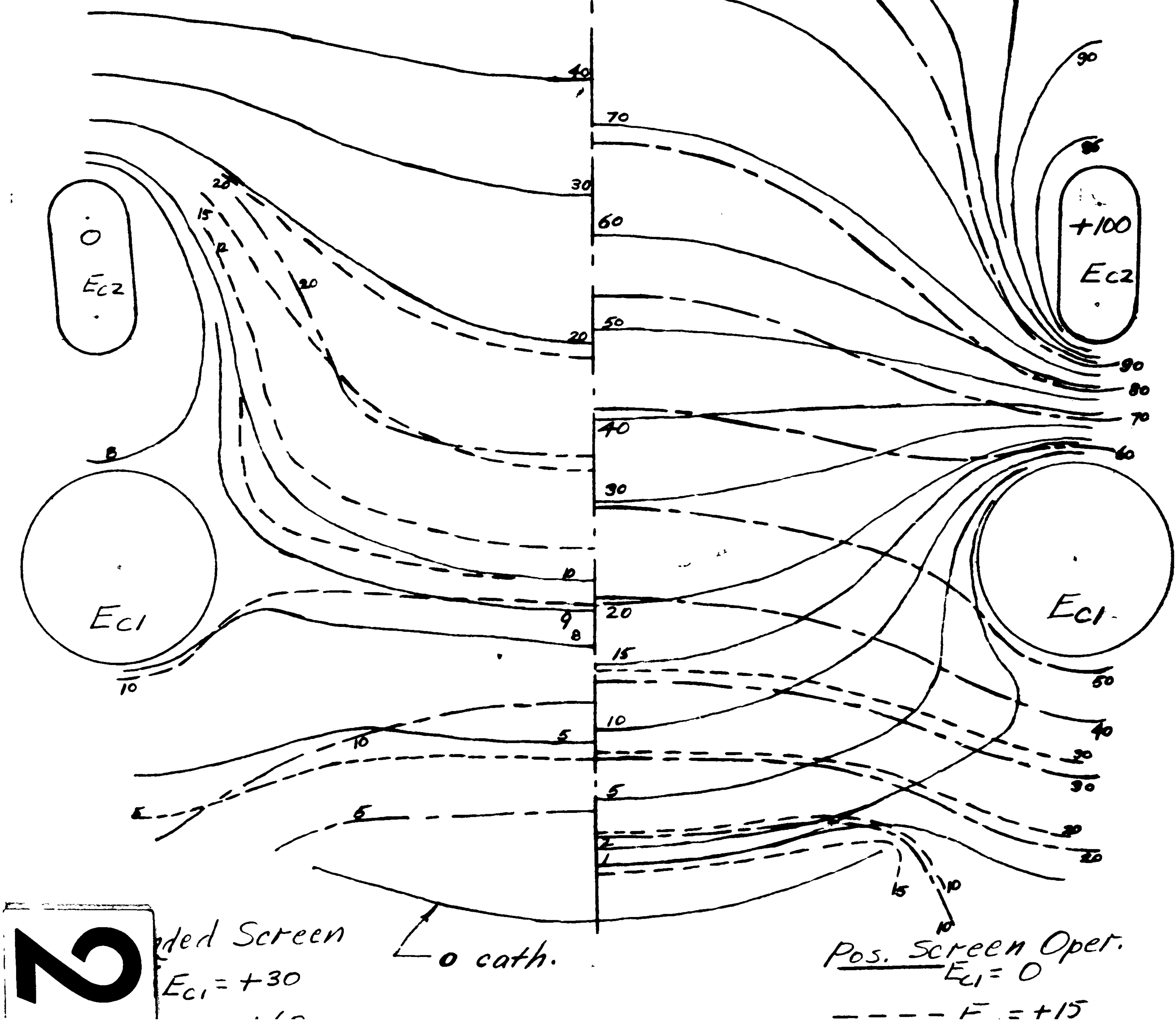

+100
E_{c2}
0
E_{c2}
E_{c1}
E_{c1}
0 cath.
...ded Screen
$E_{c1} = +30$
Pos. Screen Oper.
$E_{c1} = 0$
$E_{c1} = +15$

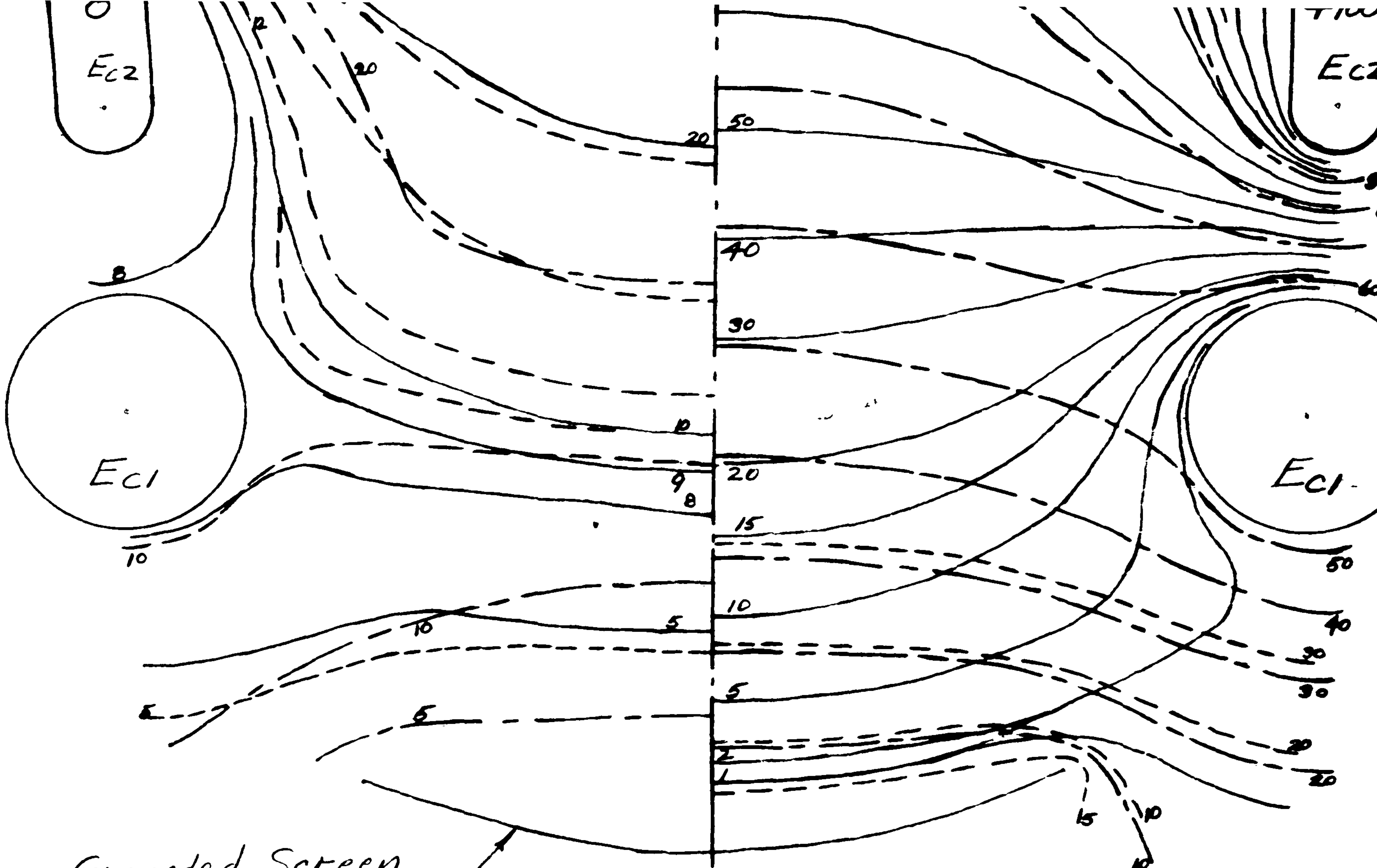

Grounded Screen Oper.
—— $E_{c1} = +30$
- - - - $E_{c1} = +60$
—·— $E_{c1} = +90$

Pos. Screen Oper.
—— $E_{c1} = 0$
- - - - $E_{c1} = +15$
—·— $E_{c1} = +30$

Des. 4
Flattened Screen
Rods

Fig. 20

3

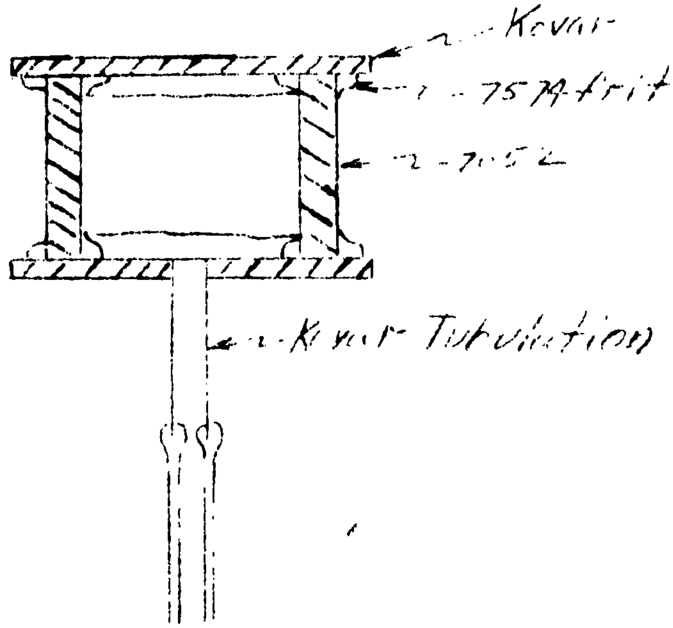

Test Frit Seal
XD32

Fig. 22

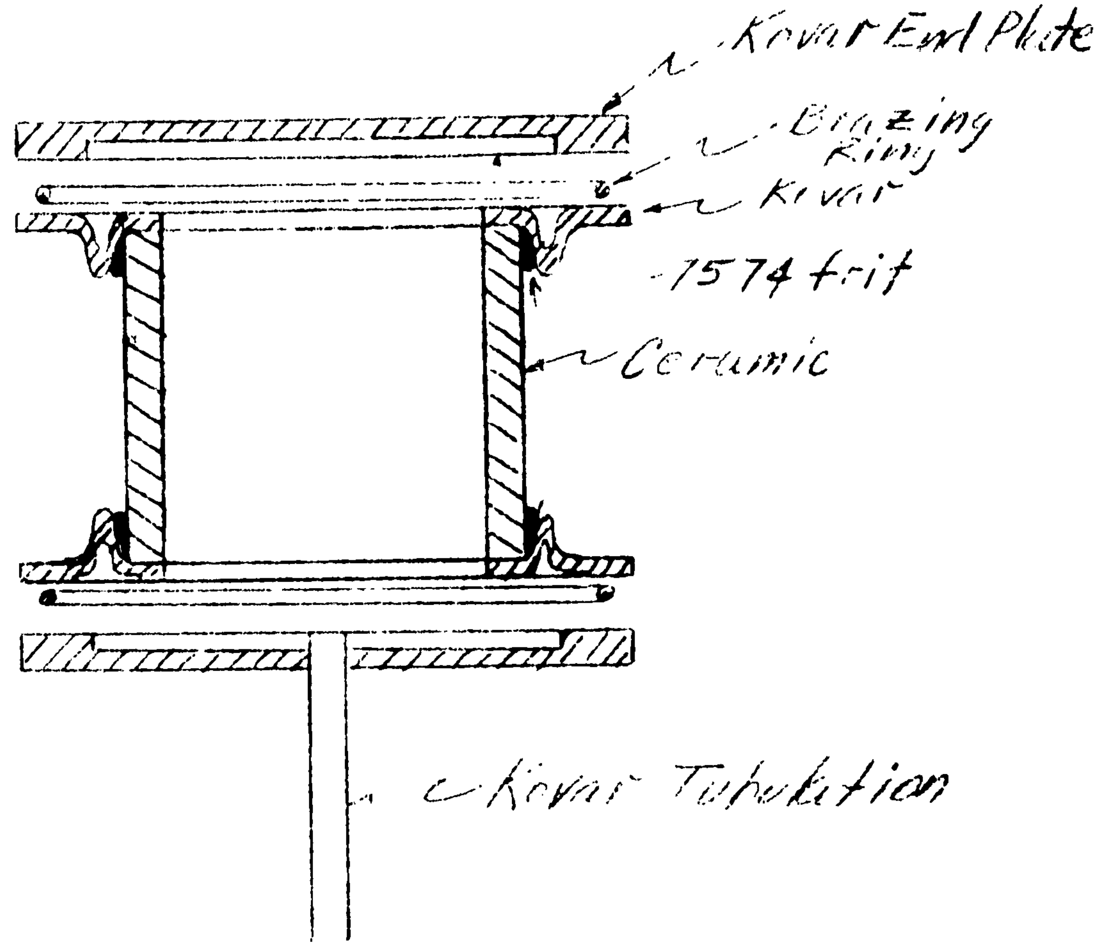

Test Metal-Ceramic Seal
XD 32

Fig. 23

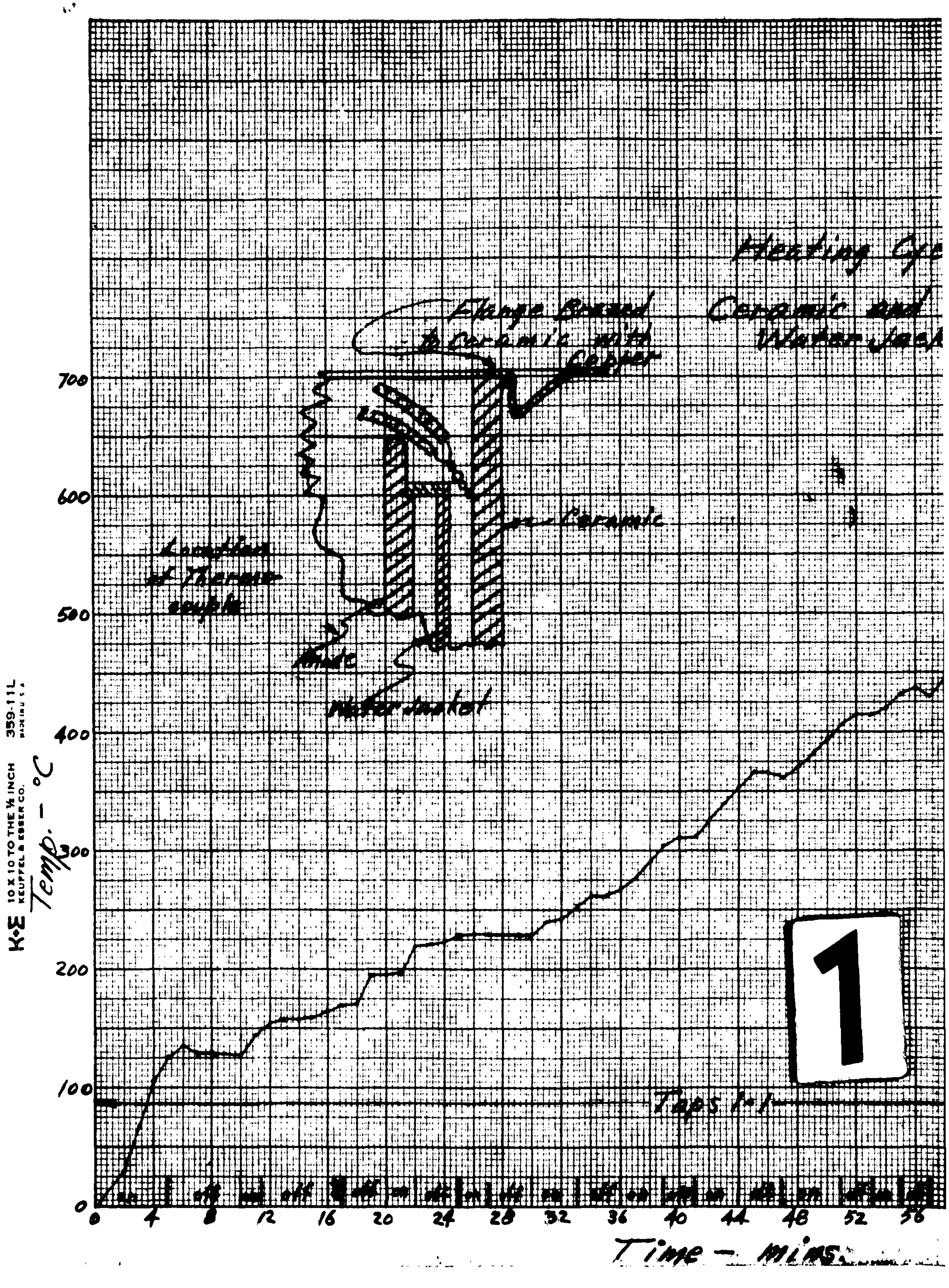

Flange Brazed to Ceramic with Copper
Ceramic
Location of Thermocouple
Anode
Water Jacket
Taps 1-1
Temp. - °C
700
600
500
400
300
200
100
0
0
4
8
12
16
20
24
28
32
36
40
44
48
52
56
Time - mins.
1
K&E 10 X 10 TO THE ½ INCH KEUFFEL & ESSER CO. 359-11L

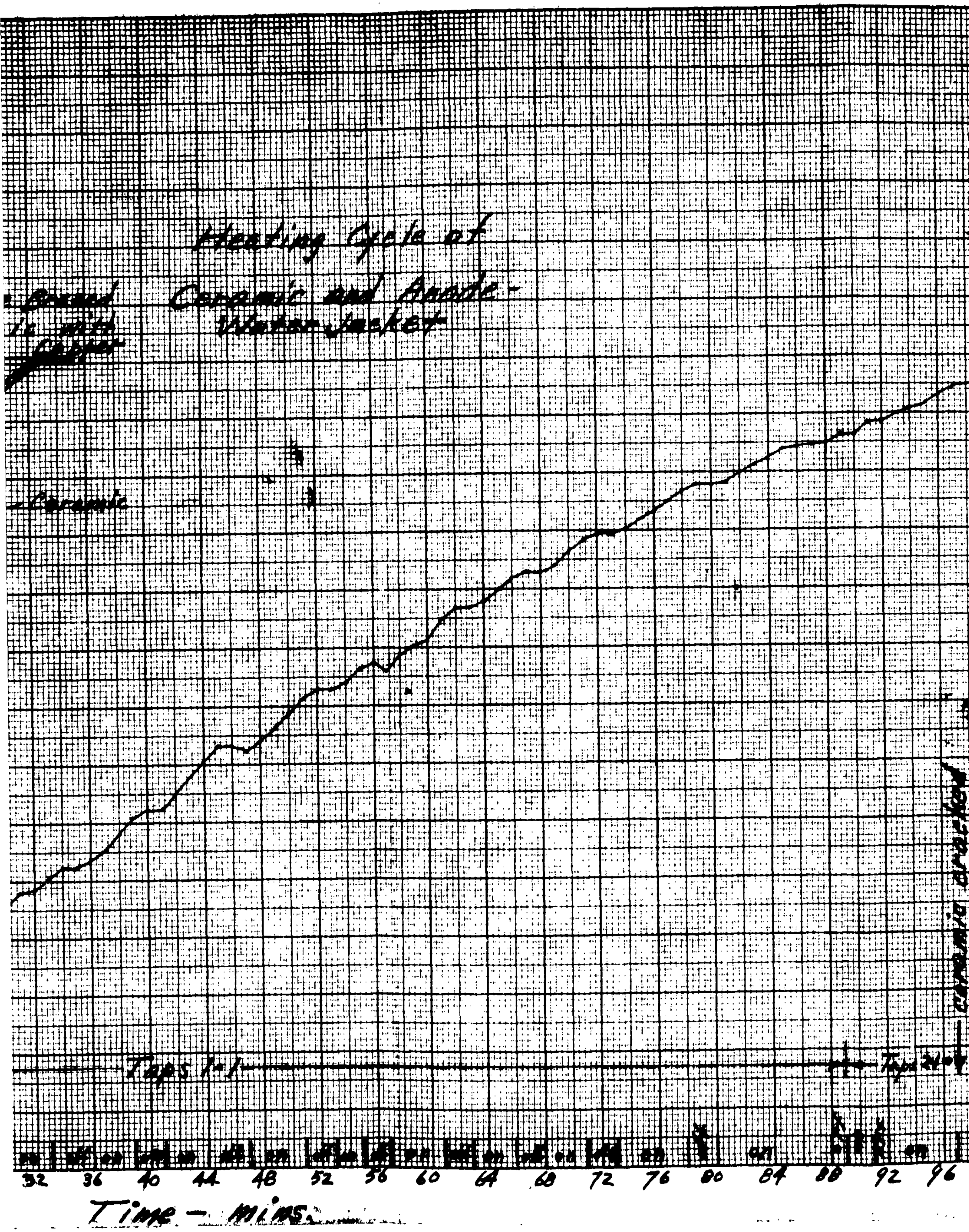

Heating Cycle of
Ceramic and Anode-
Water Jacket
Ceramic
Taps 1-1
Taps 2-1
ceramic cracked
on
off
32
36
40
44
48
52
56
60
64
68
72
76
80
84
88
92
96
Time - mins.

2

Fi

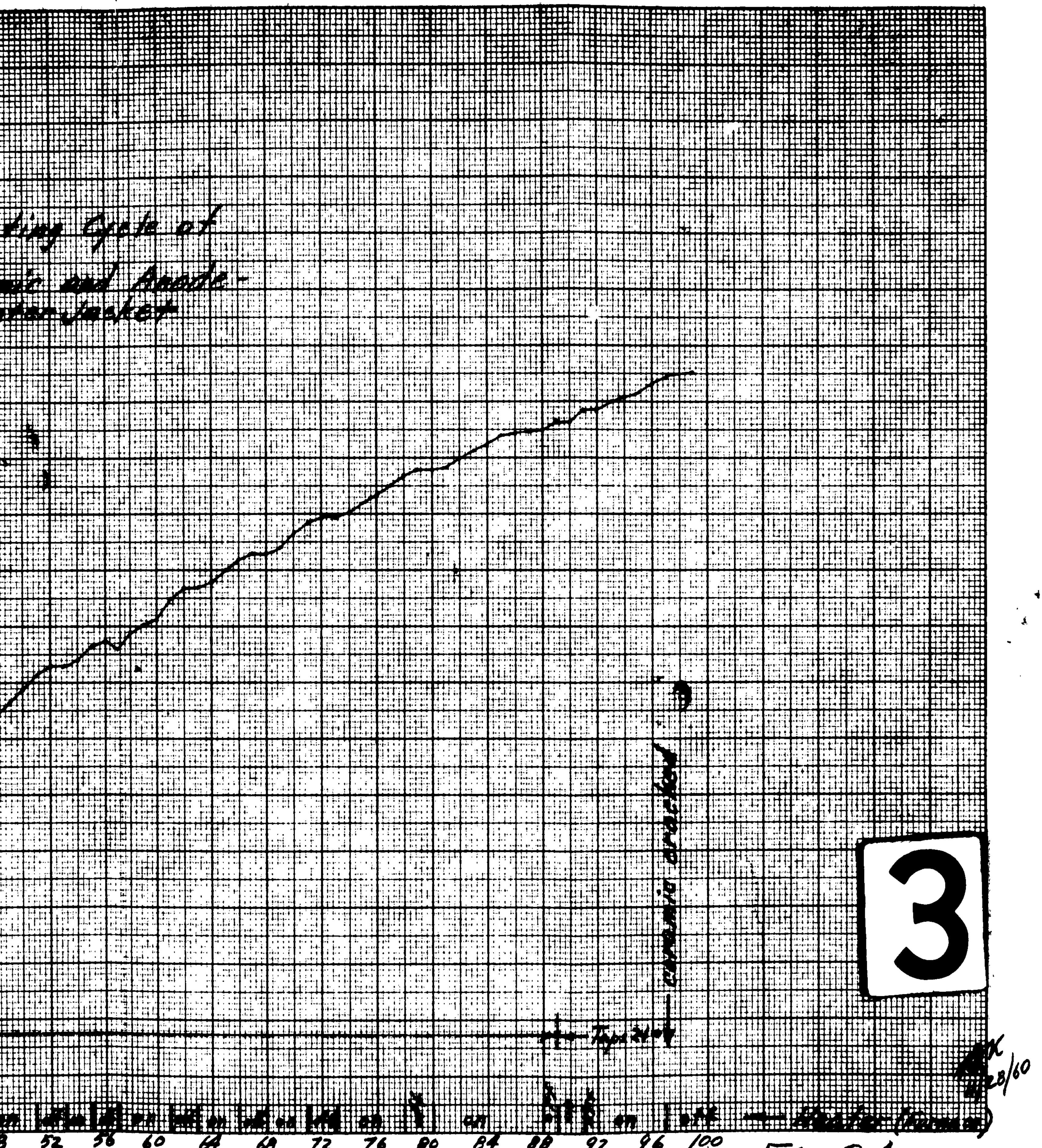

Fig. 24

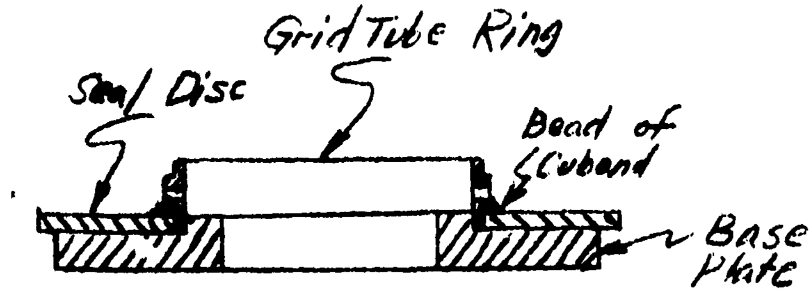

Seal Disc & Grid Tube Ring on Base Plate
Fig. 25

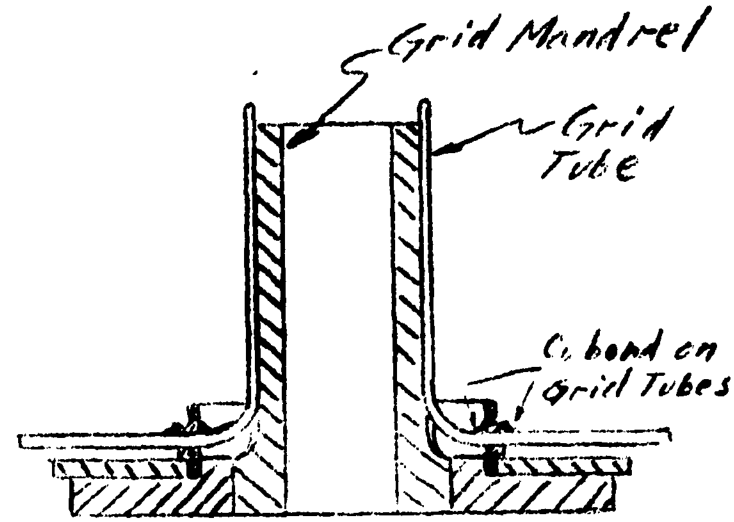

Grid Tubes in Place
Fig. 26

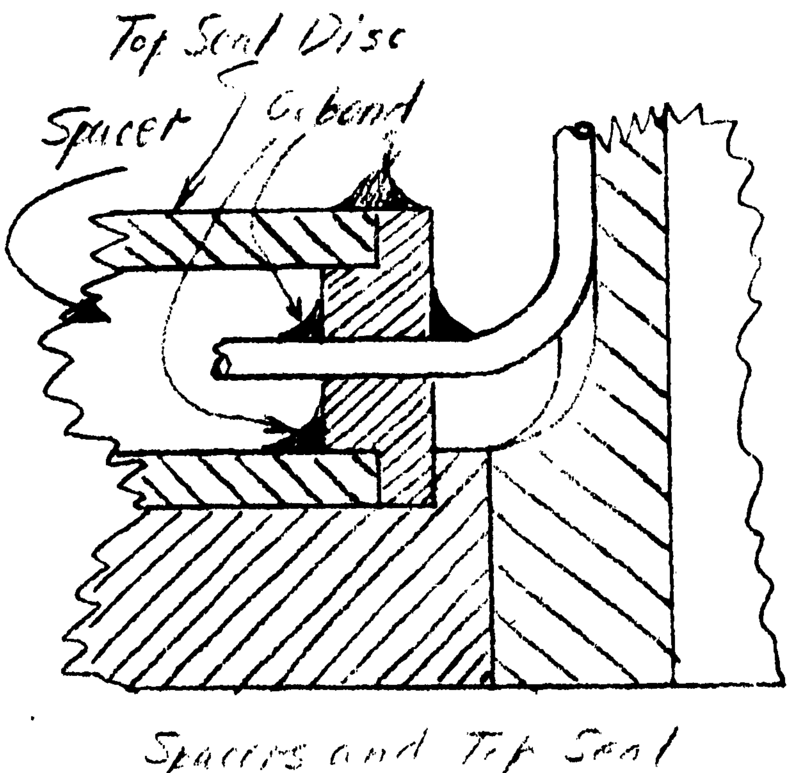

Spacers and Top Seal Disc in Place
Fig. 27

Assembly of a Grid

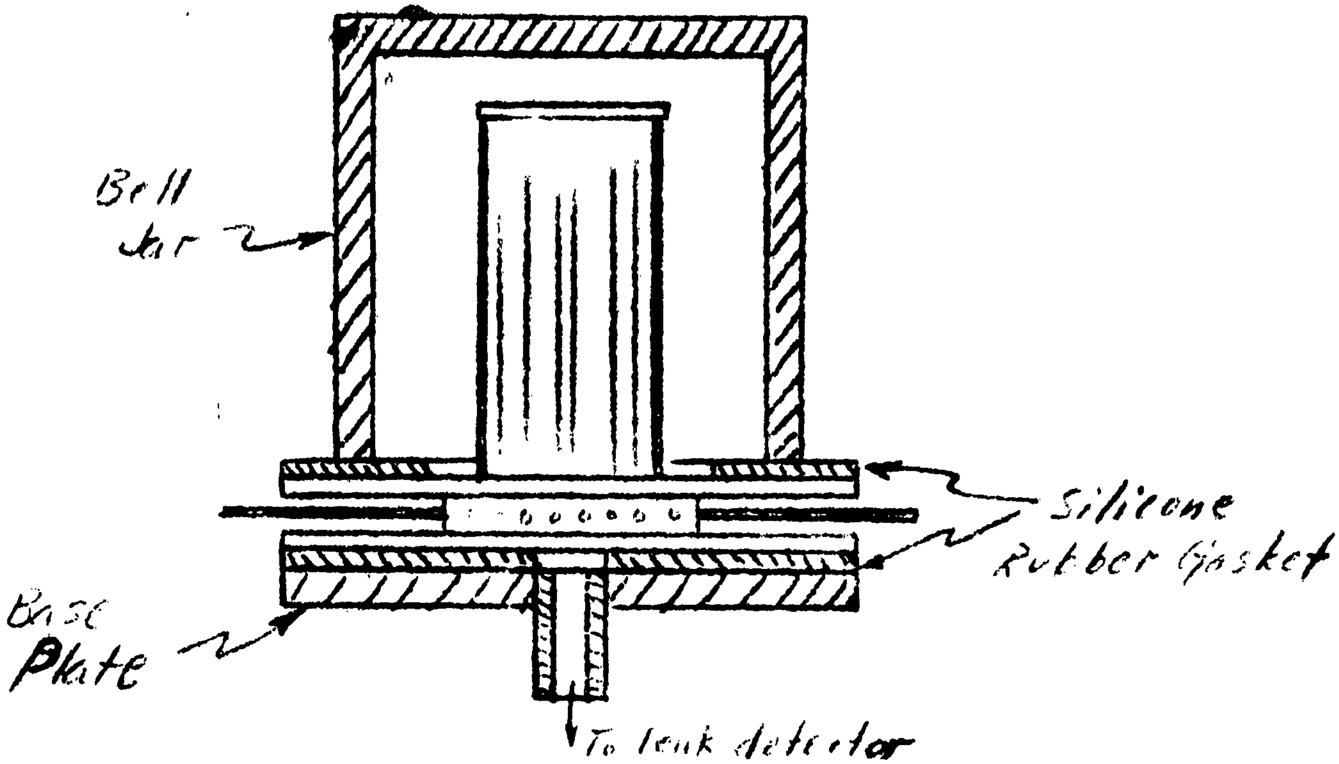

Leak Checking Grid

Fig. 26

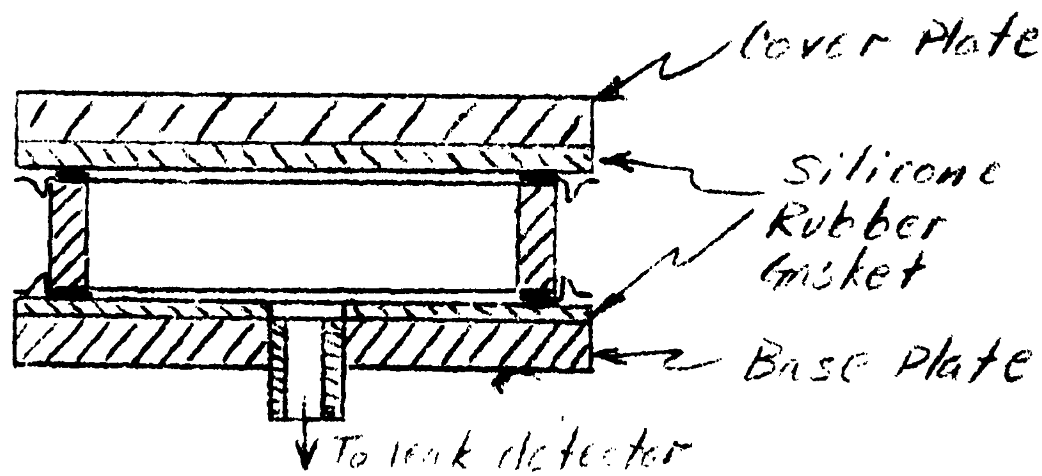

Leak Checking Ceramic-Metal Seals

Fig. 29

Distribution List for Contract AF30(602)-2027-RADC-TR-61-116

	No. of copies
RADC (RALTP)	10
RADC (RAAP)	1
RADC (RAALD)	1
ROAMA (ROZMSTT)	1
RADC (RAIS/Mr. Malloy)(For: Flt Lt Tanner) Griffiss Air Force Base, New York	1
Signal Corps Liaison Officer RADC (RAOL/Capt Norton) Griffiss AFB, NY	1
AU (AUL) Maxwell AFB Alabama	1
ASD (ASAPRD) Wright-Patterson AFB Ohio	1
Chief, Naval Research Lab ATTN: Code 2021 Washington 25, D.C.	1
Air Force Field Representative Naval Research Laboratory ATTN: Code 1010 Washington 25, D.C.	1
Commanding Officer USASRDL ATTN: SIGRA/SL-ADT Ft. Monmouth, New Jersey	1
Chief, Bureau of Ships ATTN: Code 312 Main Navy Bldg Washington 25, D. C.	1
Office of the Chief Signal Officer Dept of the Army ATTN: SIGRD Washington 25, D.C.	1
AFPR - Lockland Br. - GE Co. PO Box 91, Cincinnati, 15, Ohio	1
Chief, AF Section MAAG Germany Box 810 - APO 80 New York, New York	1

AFSC (SCSE)
Andrews AFB
Washington 25, D.C. 1

ASTIA (TIPCA)
Arlington Hall Station
Arlington 12, Virginia 10

OASD (R&E) Rm 3E1065
The Pentagon
ATTN: Technical Library
Washington 25, D. C. 1

Advisory Group on Electron Devices
346 Broadway
New York 13, New York 2

Commanding Officer
U.S. Army Signal R&D Lab
ATTN: L.N.Heynick SIGRA/SL-PRT
Ft. Monmouth, N.J. 2

Chief, Bureau of Ships
ATTN: Mr. Ray Hill
Dept of the Navy
Washington 25, D.C. 1

Director
Advanced Research Projects Agency
Washington, 25, D.C. 1

ESD (CRRCPV/J Bloom)
L.G. Hanscom Field
Bedford, Mass. 1

General Electric Research Lab.
ATTN Dr. R. Bondley
Schenectady, New York 1

Litton Industries
ATTN: Dr. J. Hull
San Carlos, California 1

Cornell University
ATTN: Dr. C. Dalman
Ithaca, New York 1

Radio Corporation of America
Power Tube Division
Lancaster, Penna. 1

Westinghouse Electric Corporation
Friendship International Airport
P.O. Box 1897
Baltimore, 3, Maryland 1

Sylvania Electric Products Inc. ATTN: Dr. R. Palmatur Emporium, Penna.	1
ITT Laboratories ATTN: Mr. R. Deutsch Nutley, New Jersey	1
Westinghouse Electric Corporation ATTN: Dr. Gene Feaster P.O. Box 284 Elmira, New York	1
Machlett Laboratories ATTN: Mr. R. Nelson Springdale, Connecticut	1